Predictability of Time Averages:

Part I: Dynamical Predictability of Monthly Means

Part II: The Influence of the Boundary Forcings

J. Shukla

Laboratory for Atmospheric Sciences
NASA/Goddard Space Flight Center
Greenbelt, Maryland 20771

Summary of lectures given at the European Centre for Medium Range Weather Forecasts, Reading, England. Seminar on "Problems and Prospects in Long and Medium Range Weather Forecasting," September 14-18, 1981.

Predictability of Time Averages:

The Influence of the Boundary Forcings

J. Shukla

Laboratory for Atmospheric Sciences
NASA/Goddard Space Flight Center
Greenbelt, Maryland 20771

Abstract

We have discussed the physical mechanisms through which changes in the boundary forcings of SST, soil moisture, albedo, sea ice, and snow influence the atmospheric circulation. The slowly changing boundary forcings can increase the predictability of monthly means because their effects on quasi-stationary flow patterns and statistics of synoptic scale disturbances appears to be potentially predictable. Changes in the boundary forcings produce changes in the moisture sources and diabatic heat sources which in turn change the atmospheric circulation. The magnitude and the structure of the atmospheric response due to changes in any boundary forcing depends upon the existence of a suitable large scale flow which can transform the boundary forcing into a three dimensional heat source, which in turn can change the large scale flow and its stability properties. The structure of the large scale flow also affects the propagation characteristics of the influence which determines whether the effect is local or away from the source.

We have presented results of numerical experiments conducted with the GLAS climate model to determine the sensitivity of the model atmosphere to changes in boundary conditions of SST, soil moisture, and albedo over limited regions. It is found that changes in SST and soil moisture in the tropics produce large changes in the atmospheric circulation and rainfall over the tropics as well as over mid-latitudes. Although the area occupied by the land surfaces is small compared to the ocean surfaces, the fluctuations of soil moisture can be very important because the diabatic heat sources have their maxima over the land, and therefore, even small fluctuations of soil moisture can produce large changes in the total diabatic heating field. The natural variability due to day to day weather fluctuations is very large in the middle latitudes, and therefore, changes in the mid-latitude atmospheric circulation due to changes in the boundary

forcings at middle and high latitudes have to be quite large to be significant. It is suggested that large scale persistent anomalies of SST, snow and sea ice, under favorable conditions of large scale flow, can produce significant changes in the mid-latitude atmospheric circulation. It is also likely that time averaged mid-latitude circulation can have additional predictability due to the influence of tropical boundary forcings.

We have also presented observational evidence to show that interannual variability of atmospheric fluctuations is significantly different from the intra-annual variability, and therefore, we conclude that part of the inter-annual variability is due to the influence of boundary forcings. Since the tropical spectra is found to be redder compared to the mid-latitude spectra, the tropical flows may be potentially more predictable.

1. INTRODUCTION

In a previous paper (Shukla, 1981) we examined the predictability of the initial conditions without external forcings, and it was shown that the dynamical predictability of the observed planetary wave configurations is sufficiently long that the predicted monthly means are significantly different from the monthly means due to random perturbations in the initial conditions. It was further suggested that in addition to the dynamical predictability of the monthly means there can be additional predictability due to the influence of the boundary forcings. This paper examines the influence of slowly varying boundary forcings at the earth's surface in determining the monthly mean circulation anomalies in the atmosphere. Figures 1a and 1b show the schematic distribution of sea surface temperature (SST), soil moisture, surface albedo, snow cover and sea ice. There is sufficient observational evidence to assume that the rate of change of anomalies of these boundary forcings is slower than the corresponding atmospheric anomalies, and therefore for a limited period of time (viz. a month or sometimes even a season) these can be considered as "external" forcing to the atmospheric circulation. In the present paper, we will confine our discussion only to these five boundary forcings. A discussion of the influence of truly external forcing due to solar variability is beyond the scope of the present paper. Similarly, effects of slow changes in the composition (viz. CO_2) and optical properties of the atmosphere will not be considered because they appear to be too slow to affect monthly prediction.

One straightforward approach to determining the influence of boundary conditions on monthly mean prediction could be to carry out actual forecast experiments using the observed initial and boundary conditions. To our knowledge, no such forecast experiment has yet been carried out in which the global distribution of observed boundary forcings was used. It is only recently that global

observing systems capable of determining global boundary conditions have been established, and still it is a formidable (but feasible) task to determine a global distribution of accurate boundary forcings. Another approach to determine the influence of the boundary forcings is to carry out a series of controlled sensitivity experiments with realistic general circulation models and to determine the regional distributions of time averaged response. This has been done using a variety of models and a variety of anomalous boundary forcings. A review of all such experiments carried out by many investigators is not possible in this paper. Here we summarize the results of only a few selected numerical experiments carried out with the Goddard Laboratory for Atmospheric Sciences (GLAS) climate model.

It should be pointed out that most of the numerical experiments carried out in the past were not especially designed to investigate the question of monthly predictability and, therefore, there was no detailed examination of the response during the first 30 days. The main interest was the difference in the simulated mean climate after the model has equilibrated to the altered boundary forcings. Such experiments are also quite useful for understanding the basic mechanisms and establish the role of boundary forcings in the interannual variability of monthly and seasonal means. In earlier studies, the choice of the geographical location of the anomaly (of SST or sea ice, etc.) was mostly determined by an analysis of the past observations, and naturally the past observations were analysed only for those areas for which data were conveniently available. On the basis of such observational studies and subsequent numerical experiments, several preliminary conclusions have been drawn about the possible relationships between the boundary forcing anomalies and the atmospheric circulation. These studies do not rule out the possibility that SST anomalies over other areas (hereto unexamined) will not be equally important. In fact,

it is quite likely that all the boundary forcing, if considered globally, will produce more realistic and systematic response in the atmospheric circulation. One of the main contentions of this paper is to emphasize that further sensitivity and predictability studies using observations, simple linear models and complex GCMs should also be carried out for global distributions of boundary forcing anomalies.

Before presenting the results of actual numerical experiments, we will briefly mention some mechanistic considerations which suggest a physical basis for the influence of the boundary forcings.

1) Changes in the boundary forcings directly influence the location and intensity of the diabatic heat sources which drive the atmospheric circulation. The forcing at the boundary itself is generally not sufficient to produce significant changes in the atmospheric circulation; however, under favorable conditions of large scale convergence and divergence, the boundary effects get transmitted to the interior of the atmosphere and a thermal boundary forcing gets transformed into a three-dimensional heat source which can be quite effective in influencing the dynamical circulation. The effectiveness of a boundary forcing in changing the atmospheric circulation therefore strongly depends upon its ability to produce a deep heat source and the ability of this influence to propagate away from the source. Since both of these factors are determined by the structure of the large scale dynamical circulation itself, the response of a given boundary forcing can be very different depending upon its size and geographical location, and upon the structure of the large scale circulation.

2) Boundary forcings of SST, soil moisture, surface albedo, snow and ice not only affect the heat sources and sinks, but they also affect the sources and sinks of moisture, which in turn affect the latent heat sources.

3) Existence of nonlinear multiple equilibrium states for a prescribed external forcing suggests that even weaker anomalies of boundary forcings,

under favorable conditions, can produce significant anomalies in atmospheric circulation, and therefore actual response may be stronger compared to the one estimated from linear theories.

4) It is known that the inconsistency between the observed initial conditions and the prescribed stationary forcings due to mountains and diabatic heat sources can manifest itself as erroneous propagating transient components (Lambert and Merilees, 1978; Shukla and Lindzen, 1981). It is therefore desirable that for actual dynamical prediction from observed initial conditions, the observed global distribution of boundary forcings be used correctly. This will reduce the inconsistency between the initial conditions and the forcing, and therefore can reduce the growth of error of prediction.

In Part I we examined predictability for prescribed nonfluctuating boundary forcings, and the predictability was determined by error growth rate and error saturation value. We can identify the following reasons due to which changes in boundary forcings can influence these classical predictability parameters.

a) Changes in the boundary forcings can change the intensity and geographical location of synoptic scale instabilities. For example, changes in the amplitudes and phases of planetary waves can affect the storm tracks, which can affect the error growth and predictability in a particular region.

b) Changes in the boundary forcings can alter the saturation value of the error. As described earlier, the saturation value of the error depends upon the equilibration mechanisms which are different for different circulation regimes and also for different scales of instabilities. Boundary forcings can alter the equilibration level of the dominant fluctuations, resulting in a significant change in the time averaged mean circulation. It should be pointed out that the effects can be very different for different parameters. For example, if for a given value of boundary forcing, the amplitude of the wave

disturbances is much less than its amplitude for another value of the boundary forcing, and if heavy rain or snow falls only during half of the life of each wave disturbance, and if the rate of rainfall is proportional to the intensity of the disturbance, then although the time averaged value of pressure or temperature will not be very different for two values of boundary forcing, the rainfall will be very different. This suggests that sometimes it may be quite useful to predict only the variance of a particular parameter.

2. SENSITIVITY OF MODEL ATMOSPHERE TO CHANGES IN BOUNDARY FORCINGS

In this section, we have summarized the results of several sensitivity studies carried out with global general circulation models to determine the influence of prescribed changes in SST, soil moisture, surface albedo, snow and sea ice, etc.

2.1 Sea Surface Temperature

The factors which determine the influence of sea surface temperature (SST) anomalies can be briefly summarized as follows.

(i) The magnitude and the spatial and temporal structure of the anomaly. Considering the linear response of the atmospheric system to diabatic forcing, the magnitude and the spatial scale of the anomaly can directly affect the response to the atmosphere. Large, persistent anomalies can produce a larger response than small fluctuating anomalies. The magnitude of the anomaly is also important in determining the nonlinear increase of evaporation and sensible heat fluxes.

(ii) Normal sea surface temperature. Due to the nonlinearity of the Clausius-Clapeyron equation, a 1° positive anomaly over a normal SST of 30° produces a

much larger change in saturation vapor pressure than the same 1° anomaly superimposed upon a normal temperature of 20°. It is partly for this reason that anomalies in low latitudes can produce larger responses compared to similar anomalies in middle latitudes. The final response also depends upon the background SST field.

(iii) The latitude of the anomaly. Because of the smallness of the Coriolis parameter, horizontal temperature gradients in the tropics produce a much larger thermal wind than in middle latitudes. Due to the lack of geostrophic constraint in low latitudes, thermal anomalies produce much larger convergence than in middle latitudes (Hoskins and Karoly, 1981; Webster, 1981).

(iv) Circulation regime. The potential response of a given anomaly strongly depends upon the structure and dynamics of the circulation regime in which the anomaly is embedded. For example, a warm anomaly in the areas of large scale convergence (viz. ascending branches of Hadley and Walker cells) will be more effective than a comparable anomaly in the area of divergence. Similarly, in the middle latitudes the effect of a SST anomaly will strongly depend upon the location of the anomaly with respect to the phase of the prevailing planetary wave configurations.

(v) Instability mechanism. The time required for the atmosphere to feel the effect of the SST anomaly also depends upon the most dominant instability mechanism which determines the generation of a deep heat source due to surface anomaly. In tropical latitudes where CISK is the primary driving mechanism, a conditionally unstable atmosphere may respond rather quickly to a warm SST anomaly, whereas in mid-latitudes where the primary driving mechanism is baroclinic instability a given SST anomaly would affect the vertical shear and, therefore, the growth rates of baroclinically unstable waves.

(vi) Structure of zonal flow. Once a SST anomaly has produced a heat source, the structure of the prevailing zonal flow is of crucial importance in

determining the propagation characteristics of the disturbances produced by the heat source. Tropical influences can affect the mid-latitude circulation by Rossby wave propagation or by changing the intensity of the Hadley cell and mid-latitude zonal flows which can interact with the mid-latitude thermal and orographic forcings.

In summary, the influence of boundary anomalies on the atmospheric circulation depends upon the existence of a favorable dynamical environment in which the surface forcing can be transformed into a three-dimensional heat source and the ability of this influence to propogate away from heat source. A warm anomaly in the tropics enhances evaporation and increases the moisture flux convergence which is the main contributor to the enhanced precipitation over the anomaly. Increased evaporation lowers the lifting condensation level, increases the buoyancy of the moist air, accelerates the deep convective activity, and increases the latent heating of the atmospheric column which further reduces the surface pressure and enhances moisture convergence. In the tropics, SST anomalies can also produce considerable effects away from the anomaly by modifying the areas of convergence and divergence. For example, if the intertropical convergence zone remains stationary over a very warm SST anomaly for a considerable length of time, those areas where ITCZ would have moved in its normal seasonal march will experience severe droughts. Similarly, a warm SST anomaly can change the location and intensity of the Walker circulation and enhanced ascending motion associated with the warm SST anomaly can produce reduced precipitation in the adjoining areas. This suggests that the effects of SST anomalies can be very nonlinear for particular regions, depending upon the location of the region with respect to the ascending branches of Hadley and Walker circulations. This nonlinearity can disappear for averages over very large areas. SST anomalies can also affect precipitation over distant areas by altering the moisture supply for the region.

The influence of SST anomalies for mid-latitudes is different than that for the tropics. SST anomalies in mid-latitudes, if they can produce a deep heat source, can change the quasi-stationary wave patterns which in turn can affect the location and intensity of the storm tracks. Therefore, the mid-latitude SST anomalies have a considerable potential to produce distant effects. This potential, however, is not fully realized for several reasons. The normal ocean temperature in mid-latitudes is relatively cold; the moist convection is not well organized and efficient enough to produce deep heat sources; due to strong geostrophic balance even large gradients in temperature do not produce large convergence, and finally, the natural variability of the mid-latitude atmosphere is so large that small effects due to boundary forcings cannot be distinguished from synoptic weather fluctuations.

Most of the observational and numerical studies that have been carried out so far have only looked into the influence of regional SST anomalies. We do not have enough observational and numerical experimental results to describe the effects of hemispheric and global scale SST anomalies. We hope that future studies will examine the effects of very large scale SST anomalies. Here we shall present the results of a few sensitivity studies carried out by global general circulation models to determine the influence of regional SST anomalies.

2.1.1. Effect of Arabian Sea sea surface temperature anomaly on Indian monsoon rainfall

Several observational studies have suggested that SST anomalies over the Arabian Sea can be one of the important boundary forcings which determine the monsoon rainfall and therefore affects its interannual variability. A numerical experiment was carried out by Shukla (1975) using the Geophysical Fluid Dynamics Laboratory (GFDL) model to test the validity of observed correlations. A cold SST anomaly shown in Figure 2a (anomaly run) was imposed over the climatological

SST (control run) and the model was integrated for both cases. Figure 2b shows the model simulated rainfall of the Indian region for anomaly and control integrations. It is found that due to cold SST anomalies over the Arabian Sea monsoon rainfall is reduced over India. A similar experiment was carried out by Washington et al., (1977) using the National Center for Atmospheric Research (NCAR) model; however, their results were contrary to both the numerical results of the GFDL model and observed correlations. We have examined the results of the Goddard Laboratory for Atmospheric Sciences (GLAS) climate model in which a warm SST anomaly very similar in pattern to the anomaly shown in Figure 2a was used. Figures 3a and 3b show the model simulated rainfall for anomaly and control runs averaged over two areas shown in Figure 3c. The GLAS model was integrated for three different initial conditions, but very similar SST fields over the Arabian Sea. The curves labeled ANOMALY in Figures 3a and 3b show the average rainfall for three anomaly runs and the vertical bars denote the standard deviation among the three runs. It can be seen that warm SST anomalies over the Arabian Sea, as prescribed in these experiments, can produce enhanced monsoon rainfall over India. We do not know, however, whether such large anomalies are actually observed.

The apparent disagreement between the results of Washington et al., (1977) using the NCAR model, and our results using the GFDL and GLAS models can be explained by examining the low level monsoon flow as simulated by the three models and shown in Figure 3d. The low level monsoon flow as simulated by GFDL and GLAS models are more realistic compared to the NCAR model. In the NCAR model simulation, the air parcels flowing over the Arabian Sea hardly reach the Indian region as there is a strong but unrealistic southward flow before the monsoon current reaches the Indian coast. This could be one of the possible reasons why the NCAR model did not show significant response over India. This

example illustrates the importance of a realistic simulation of the mean climate by the dynamical model used for the sensitivity studies. In order to be able to detect the effects of changes in the boundary forcings, and for the possible use of such models for prediction of time averages, the model should be able to simulate the mean climate accurately.

2.1.2. Effect of tropical Atlantic sea surface anomalies on drought over northeast Brazil

Moura and Shukla (1981) examined the monthly mean SST anomalies over the tropical Atlantic during March and rainfall anomalies over northeast Brazil during March, April and May. They found that the most severe drought events were associated with the simultaneous occurrences of warm SST anomalies over the north tropical Atlantic and cold SST anomalies over the south tropical Atlantic. They also carried out numerical experiments to test the sensitivity of the GLAS climate model to prescribed SST anomalies over the tropical Atlantic. It was found that the SST anomaly patterns, which resemble the observed ones during drought years, produced an intensified convergence zone (ITCZ), enhanced rainfall and low level cyclonic circulation to the north, and reduced rainfall and anticyclonic circulation to the south.

Figure 4a shows the SST anomaly used for the numerical experiment; the magnitude was chosen to be comparable to the maximum values observed during the 25 year period (1948-72). Figure 4b shows the 15 day running mean time series of daily rainfall averaged over the areas A and B (shown in Figure 4a) for control and anomaly runs. Area A includes the region of warm SST anomaly and area B contains the northeast Brazil region and the neighboring oceans with the cold SST anomaly. The rainfall over area A increases due to the warm SST anomaly and a shift of the ITCZ occurs from area B in the control run to area A in the anomaly run. Although the difference in rainfall is not systematic

after 60 days, for days 20-60 the anomaly run has consistently less rainfall than the control run over northeast Brazil region. Figure 4c shows the difference of the first 60 day mean meridional circulation averaged between 50°W and 5°E. The anomalous meridional circulation shows an ascending branch with maximum vertical motions between 5° and 10°N and a descending branch to the south of the equator. A thermally direct local circulation is established with its ascending branch at about 10°N and its descending branch over northeast Brazil and adjoining oceanic regions. The driving for the anomalous circulation is provided by convection and latent heating associated with warmer SST anomalies over the northern tropical Atlantic, and cooling associated with colder SST anomalies in the southern tropical Atlantic. The combined effects of thermally forced subsidence and the reduced evaporation and moisture flux convergence produces severe drought conditions over northeast Brazil. It should be pointed out that descending motion influences a larger region to the east and west of northeast Brazil, however, the effect is most seriously felt over northeast Brazil. It was also noticed that the anomalous meridional circulations exhibited significant changes in the middle latitudes of both hemisphere.

Figure 4d shows the autocorrelation function for SST anomalies at 15°S, 5°W and at 15°N, 45°W. The strong persistence of SST anomalies in these two areas suggests the potential for prediction of drought over northeast Brazil.

2.1.3 Effect of Equatorial Pacific SST Anomaly on Tropical and Extratropical Circulations.

Horel and Wallace (1981) and Rasmusson and Carpenter (1982) have presented observational evidences of remarkable relationships between SST anomalies in tropical Pacific and a variety of atmospheric fluctuations including the Southern Oscillation and the Northern Hemispheric middle latitude circulations. "Warm episodes of equatorial Pacific SST anomalies are associated with the negative

phase of the Southern Oscillation, weakening of easterlies in equatorial central Pacific, enhanced precipitation at equatorial stations east of 160°E, an intensified Hadley cell in Pacific sector, and a deepening and southward displacement of the Aleutian low" (Horel and Wallace, 1981). Analyses by Rasmusson and Carpenter (1982) have shown that during the month of December, a small warm SST anomaly appears along the Peru coast which rapidly increases to its peak value along the Peru coast during March and April of the following year. In the month of February of the following year, the warm SST anomaly disappears rapidly along the Peru coast, but the warmest SST anomalies are observed in equatorial central Pacific. It is these warm SST anomalies over the central Pacific, which occur over a climatologically warmer ocean surface which is also an area of large scale convergence, that produce a deep tropical heat source whose effects can propagate to the extratropical latitudes. Therefore, although the signal for a warm SST anomaly during February of a given year could be traced back to warm SST anomalies over the Peru coast fourteen months earlier, it is the enhanced heating associated with the SST anomaly during February that produces significant changes in the winter circulation of the northern mid-latitudes. Hoskins and Karoly (1981) used a multi-level linear primitive equation model to show that diabatic heat sources in the tropical regions can produce significant stationary responses in the middle latitudes if the zonal flow is favorable for the propagation of Rossby waves.

Shukla and Wallace (1983) have conducted sensitivity experiments with the GLAS climate model to study the response of SST anomalies in equatorial Pacific. Figure 5a shows the average of SST anomalies observed during the months of November, December and January of 1957-58, 1965-66, 1969-70, and 1972-73, provided to us by Dr. Rasmusson of NOAA. The GLAS climate model was integrated with (anomaly run) and without (control run) the SST anomalies shown in Figure 5a.

Figure 5b shows the difference (anomaly minus control) field for 300 mb geopotential height averaged for days 11-25. It is seen that a difference of about 300 meters over North America and about -90 to -150 meters over Pacific and Atlantic is in agreement with results of observational studies as well as the results of linear models. Upper level highs to the north of the anomaly and a series of lows and highs further north and west are manifestations of Rossby waves propagating from the heat source. An examination of day-to-day changes from day 1 through 30 showed that this particular pattern was already established during days 5-10. However, it takes several days before model physics can generate a deep heat source above the warm SST anomaly. It should be pointed out that although the results of the linear models and this general circulation model are similar, there is a basic difference for their applicability to dynamical prediction of monthly means. The simple models prescribe the diabatic heating fields, whereas the general circulation model generates a diabatic heating field due to the presence of the warm SST anomaly, and therefore for a model to be useful as a prediction tool, its physical parameterizations must be able to transform the surface boundary forcing into a deep heat source. As mentioned earlier, the propagation of the tropical influences depends upon the structure of the zonal flow (influences cannot propagate across the zero wind line). In the present experiment, although the SST anomaly was centered right over the equator, the zonal flow was favorable for the tropical effects to propagate to middle latitides.

We have also examined the changes in the model simulated Hadley and Walker cells due to the prescribed SST anomalies. Figure 5c shows the difference between the Hadley cell for the anomaly and the control run averaged for days 6-25. It is seen that the zonally averaged Hadley cell intensifies due to warm SST anomalies over the equatorial Pacific. The Hadley cell over the Pacific

sector alone is intensified even more. It was also noticed that in association with stronger Hadley cells, the westerly zonal flow was also stronger between 20° and 30°N. Figure 5d shows the difference (anomaly minus control) for the model simulated Walker cells averaged between 6°N and 6°S for days 6-25. Anomalous ascending motion occurs between the longitude sector 160°E - 160°W and descending motion occurs between the longitudes 140°E - 160°E. This is consistent with the observational evidence of enhanced precipitation east of 160°E being associated with warm SST anomalies.

A remarkable aspect of the results of this experiment is that the prescribed SST anomaly was an algebraic mean of four different episodes and therefore the prescribed maximum warm anomaly at any grid point was perhaps less than observed during any individual year. However, it produced significant changes within the first 30 days. The results also suggest that the SST anomalies can be of importance even for medium range (5-15 days) forecasting.

2.1.4 Effect of north Pacific SST anomaly on the circulation over North America.

As it was pointed out earlier, due to the large day-to-day variability in the middle latitudes, it is difficult to detect the influence of SST anomalies. However, if a large scale SST anomaly of large magnitude persists for a long time, it can also produce significant effects in the midlatitude circulation. During the fall and winter of 1976-77, SST in the north Pacific was characterized by abnormally cold temperatures in the central and western portions of the northern Pacific with a warm pool located off the west coast of the U.S. (Figure 6a). Namias (1978) has suggested that the northern Pacific SST anomalies may have been one of the multiple causes of the abnormally cold temperatures in the eastern North America during the 1976-77 winter. We have carried out numerical experiments with the GLAS climate model to test this hypothesis. It should be noted that although the pattern of the SST anomalies observed during January

1977 was similar to the one shown in Figure 6a, the magnitude of the anomaly was only slightly more than half of the magnitude shown in the figure. It should also be pointed out that during January 1977 a warm SST anomaly over the equatorial Pacific was also observed and it is likely that the circulation of North America could have been affected by combined effects of both anomalies. In this experiment, we have attempted to determine the effect of north Pacific SST anomaly only. We have integrated the GLAS climate model with six different initial conditions and climatological mean SST (control run) and for two of these initial conditions we have also integrated the model with imposed SST anomalies (anomaly run). The results that we show here are the differences between an average of six control runs and two anomaly runs.

Figure 6b shows the difference (anomaly minus control) for the 700 mb temperature averaged for days 15-45. As expected, negative temperature anomalies are found over the maximum negative SST anomaly and a warm 700 mb temperature anomaly is found over the warm SST anomaly. The most remarkable feature of this map, however, is the occurrence of two other centers of negative 700 mb temperature anomaly, one along 75°W and the other along 70°E. The cold 700 mb temperature anomaly over northeast North America is of largest magnitude. This feature suggests a planetary wave response due to north Pacific SST anomaly. The ratio between the temperature differences shown in Figure 6b and the standard deviation among the six control runs with climatological SST shows (Figure 6c) that the colder temperatures at 700 mb over northeast North America are as significant as the ones over the cold SST anomaly. The difference map (anomaly minus control) for the 500 mb geopotential height field shows (Figure 6d) that colder temperatures over northeast North America were due to anomalous northerly flow of cold air which in turn was caused by anomalous positive

geopotential height anomalies to the west and negative geopotential height anomalies to the east. There are discrepancies between the simulated and the observed anomaly during the winter of 1977, because the response is one quarter wavelength out of phase. However, a detailed examination of the day-to-day evolution of the flow for the control and anomaly runs revealed that a persistent blocking type of flow configuration existed in the anomaly run for more than 15 days (Chen and Shukla, 1983). Such persistent blocks did not occur in the control case. We are not quite sure if the blocking event generated in the anomaly run was due to presence of the SST anomaly. However, on the basis of the results of these experiments and the results of several observational studies, it is our conclusion that for favorable structures of the large scale flow, large scale SST anomalies in the mid-latitudes can be important in determining the anomalies of the mid-latitude circulation.

2.2 Soil Moisture

The annual average rainfall for the global continents is estimated to be about 764 mm of which 35-40% (266 mm) runs off to the oceans (Baumgartner and Reichel, 1975). Assuming no secular trends in the annual mean global soil moisture, this suggests that the annual and global mean evaporation from the land surfaces alone is more than 60% of the annual and global mean precipitation over the land. The percentage is even higher during the local summer for several regions. This suggests that the evaporation from the land surfaces is a very important component of the global water budget and hydrological cycle. However, it does not necessarily follow that the water evaporated from the land is important in determining the rainfall over the land. For example, all the water evporated from the land could be advected away to the oceans before it recondenses and rains. In that case, it will affect the moisture budget

and evaporation only over the oceans, which in turn will, of course, affect the moisture supply for rainfall over the land. In order that the evaporation from the land affects the rainfall over the land, it is necessary that the prevailing dynamical circulation be such that the land evaporated moisture recondenses and falls as rain before being advected away. That will depend upon the geographical location of the region under consideration, the prevailing advective velocity, the structure and intensity of the convergence field, and the vertical distribution of moist static energy which determines the nature of moist convection.

The role of soil moisture is twofold. First, it determines the rate of evaporation and, therefore, the moisture supply, and second, it influences the heating of the ground which determines the sensible heat flux and affects the dynamical circulation by generation or dissipation of heat lows. The interaction between the heat lows, generated by solar heating of the ground in the absence of soil moisture, and associated circulation and rainfall is further complicated by the fact that the maintenance and the intensification of the low pressure areas is largely influenced by the latent heat of condensation. For example, if the soil is saturated with water, and the evaporation is equal to the potential evapotranspiration, there will be maximum possible supply of moisture to the atmosphere. Whether increased evaporation will also increase the rainfall will depend upon the structure of dynamical circulation and prevailing flow patterns. If the rate at which the moist static energy ($cpT + gz + Lq$) is advected away from the region is larger than its accumulation rate, it will not lead to any increase in the rainfall. For the other extreme situation, when the soil is completely dry, and there is no evaporation from the land, there may be a reduction in the rainfall due to reduced evaporation. However, if the heating of the land produces intense low pressure areas which can converge

moisture from the surrounding oceans, the rainfall may not necessarily decrease, and if the convergence of moisture is large enough rainfall may even increase. The mechanism will cease to operate, however, once the rain starts falling because the soil will not be dry anymore.

Since the net diabatic heating of a vertical atmospheric column is maximum over the tropical land masses (Figures 7a and 7b), it is quite likely that small fractional changes in these tropical asymmetric heat sources could produce considerable changes in the planetary scale circulations of the tropical as well as the extra-tropical atmosphere. Therefore, in spite of relatively smaller earth surface area being covered by land, soil moisture effects could be as important as SST anomaly effects. It should be noted, however, that the soil moisture effects strongly depend upon the season and latitude because during the winter season in high latitudes, solar radiation reaching the ground is not large enough to be important for surface energy budget. We summarize here the results of two numerical experiments, carried out by Shukla and Mintz (1982) which have demonstrated that evaporation from land can significantly affect the rainfall over land.

2.2.1. Influence of global dry-soil and wet-soil on atmospheric circulation

We have carried out two 60 day integrations of the GLAS climate model: in one case, there is no evaporation from the land surface ("dry-soil" case) and in the other case the evaporation from the land is equal to the model calculated potential evapotranspiration ("wet-soil" case). These two cases are qualitatively similar to no vegetation and completely vegetated earth surface. For simplicity of interpretation of the results, albedo of the soil was not altered for the two experiments.

Figure 7c shows the global maps of mean July rainfall difference (dry soil-wet soil). Over most of the continental regions, with the exception of the

major monsoon regions, July rainfall for dry-soil case has decreased (by about 40-50%) compared to the wet-soil case. This shows that the evaporation from the land is an important component of the rainfall over the land. The exception over India is even more interesting because the solar heating of land for dry-soil produced such intense low pressure and convergence that the loss of moisture from land evaporation was more than compensated by the increased moisture flux convergence from the neighboring oceanic region. The increased moisture flux convergence leads to increased heating of the vertical air column due to the latent heat of condensation which maintains and intensifies the surface low. This happened prominently for the unique monsoonal circulation over India for which oceanic moisture was brought in from the ocean by the monsoon current. This could also occur in several other regions with monsoonal flow patterns but perhaps the coarse grid resolution of the model could not resolve the local influence over other regions.

Figure 7d shows the ground temperature difference (dry soil-wet soil) for July. Ground temperatures for dry-soil are warmer by more than 20°-30°C. For the dry-soil case, most of the radiation energy goes to heat the ground and to increase the sensible heat flux, whereas, for the wet-soil case, most of the radiation energy goes to evaporate the water which can later release the latent heat of condensation and heat the vertical air-column.

Figure 7e shows the surface pressure difference (dry soil-wet soil) for July. There are intense low pressure areas over the continents for dry-soil and the mass removed from over the land is found to produce high pressure areas over the oceans. The location and the intensity of the high pressure areas over the oceans are determined by the nature of dynamical circulations, the most important of which are the mid-latitude stationary wave response to a highly anomalous diabatic forcing, and the modified Hadley and Walker circulations

due to changes in the intensity and location of the tropical heat sources.

We have also calculated the natural variability (not shown) of the GLAS model and it should suffice to say that the changes shown here for dry-soil and wet-soil are far too large to be confused with the model variability due to internal dynamics.

Since the spatially and temporally averaged rainfall over any region depends upon evaporation (which depends upon soil moisture), and vertical distribution of the moisture flux convergence (which depends upon the nature of dynamical circulation, which, in turn is determined by the direct heating of the ground and vertical distribution of latent heat of condensation), it is not possible to establish simple universal relationships between soil moisture, atmospheric circulation and rainfall. Such relationships strongly depend upon the dynamical circulation in the region under consideration. If the moisture over land is rapidly advected away to oceans, it is unlikely that the local evaporation from land will be an important contributor to the rainfall. On the other hand, the intensity and life cycle of a tropical disturbance which moves over land can strongly depend upon the wetness of the ground. It is therefore necessary to utilize realistic physical models of the earth-atmosphere system to determine the sensitivity of climate to fluctuations of soil moisture. The experiments reported in this study are extreme examples to highlight the maximum bounds of impact and to show that the importance of soil moisture and vegetation for rainfall over any particular area should be calculated by including the combined effects of dynamical circulation and orographic and oceanic forcing. It has also been reported that soil moisture boundary forcing can be an important factor for medium range (5-15 day) forecasting of rainfall and circulation. (See Mintz (1982) for a review of several numerical experiments.)

2.3 Surface Albedo.

Charney et al. (1977) had suggested that changes in the surface albedo can produce significant changes in the local rainfall and atmospheric circulation. They pointed out that this effect can be especially important in the desert margin regions of subtropics. Charney et al. used an earlier version of the GLAS model in which the surface albedo was increased by 30% for the Sahel, the Thar Desert (India), and the western Great Plains of the U.S. They found that precipitation over the albedo anomaly regions was reduced by 10-25% within the first 30 days. An increase in the surface albedo reduced the solar radiation reaching the ground, which in turn reduced evaporation from the ground. These reductions in evaporation and cloudiness increased the solar radiation reaching the ground, thus partly compensating for reduction in solar radiation due to increased albedo. However, since reduction in the cloudiness also caused reduction in the long wave radiation emitted back to the surface from the cloud base, there was a net reduction in the total radiative energy coming to the ground. This caused a net reduction in evaporation, cloudiness and precipitation. Since these subtropical regions were not affected by large advective effects, the local changes in radiative and latent heating were accompanied by dynamical circulations which produced descending motion over the albedo anomaly regions. As it was pointed out by Charney et al. (1977), the net effect on the atmospheric circulation due to changes in surface albedo depends upon the relative magnitude of the time scale for advecting the moist static energy away from the region and the time scale for its generation by evaporation and convergence. If the net effect of the change in surface albedo is to reduce the sensible and latent heating of the air, it will either decrease the low level convergence and ascending motion or increase the low level divergence and descending motion. The change in the vertical velocity field in either case will dry the middle

troposphere and further reduce precipitation. These effects may not operate in areas of large scale moisture convergence or strong dynamical instabilities; however, these experiments suggested that it is quite important to give a realistic prescription of surface albedo for prediction of monthly and seasonal atmospheric anomalies.

These experiments have been recently repeated by Sud and Fennessy (1982) using the present version of the GLAS climate model which has better parameterizations for evaporation and sensible heat fluxes. Sud and Fennessy have found that the results of experiments with the present model support all the conclusions of the earlier studies by Charney et al. An increase in albedo produced a systematic decrease in rainfall over Sahel and Thar Desert. The only exception occurred for western Great Plains where the change was not large enough to be distinguished from the day-to-day variability.

2.3.1. Effect of change in albedo over northeast Brazil.

In addition to the areas chosen by Charney et al., Sud and Fennessy also examined the effect of change in surface albedo over northeast Brazil. Between 4°S and 24°S, and 32°W and 47.5°W, surface albedo for 10 model grid points was increased from about 9% to 30%. Figure 7f shows 5 day averages of model simulated total rainfall over northeast Brazil for the anomaly (increased albedo) and the control run. It is seen that the rainfall for the first 20 days decreases due to an increase in albedo. For a 5 day period from day 20-25 rainfall in the anomaly case is more than the control. But again, from day 25-45 rainfall for the anomaly case is considerably less than that for the control case. Since rainfall over northeast Brazil is sometimes affected by the penetration of Southern Hemisphere mid-latitude disturbances, the changes during day 20-25 could be attributed to extratropical variability.

2.4 Snow Cover

About a century ago, Blanford (1884) observed that, "The excessive winter and spring snowfall in the Himalayas is prejudicial to the subsequent monsoon rainfall in India." These observations were later substantiated by Walker (1910). A persistent anomaly of snow cover can affect the meridional temperature gradient and, therefore, vertical shear of the large scale flow. The monsoon circulation is characterized by reversal of the normal temperature gradient between the equator and 30°N, i.e. during the Asiatic summer monsoon season, the equator is colder than northern India. An excessive snowfall during the previous winter and spring season can delay the build-up of the monsoonal temperature gradients because most of the solar energy will be utilized for evaporating the snow or for evaporating the soil moisture due to excessive snow. A weaker meridional temperature gradient between equator and 30°N can give rise to a delayed and weaker monsoon circulation. No systematic numerical experiments have been carried out with global GCMs to determine the physical mechanisms that can affect the atmospheric circulation associated with excessive snowfall. One reason for lack of such numerical experiments is perhaps the requirement of a rather long time integration (from one season to the other) of a global general circulation model. It requires a realistic treatment of albedo as well as surface hydrology because a large and deep snow cover during winter and spring can keep the soil wet for a longer time in the coming summer, and this effect must be treated accurately. It is only recently that general circulation models have shown some success in simulating the seasonal cycle of the atmosphere, and it is hoped that more systematic studies of various snow cover feedback mechanisms will be carried out in the coming years.

Hahn and Shukla (1976) found an apparent relationship between Eurasian snow cover and Indian monsoon rainfall (shown in Figure 8). Large and persistent

winter snow cover anomalies over Eurasia can produce a colder mid-latitude troposphere in the following spring which can strengthen the upper level anti-cyclone, slow its northward movement over India, and give rise to delayed and weaker monsoon rainfall. Some recent studies by Yeh et al., (1981) have suggested that Eurasian snow cover anomalies can influence the interannual atmospheric variability of China.

Namias (1962, 1978) has proposed that positive feedback can occur between excessive snow cover on the east coast of North America and quasi-stationary circulations which can be favorable for producing more snowfall. Since the natural variability of the mid-latitude atmosphere is quite large, it is difficult to determine the contribution of snow cover anomalies in producing mid-latitude atmospheric anomalies. The possible physical processes which have the potential to influence the atmospheric circulation due to snow cover anomalies can be briefly mentioned:

(i) An increase in snow cover increases the albedo, and therefore reduces the incoming solar radiation. If there are no other feedbacks, this will produce colder temperatures, and therefore snow cover anomalies will tend to persist for a longer time. This is consistent with the observations of Wiesnet and Matson (1976) who showed that December snow cover for the Northern Hemisphere is a very good predictor of snow cover for the following January through March.

(ii) Excessive snow cover anomalies in the mid-latitudes can produce anomalous diabatic heat sources which in turn can produce anomalous stationary wave patterns which can alter storm tracks and their frequency.

(iii) Persistent snow cover anomalies can change the components of the heat balance of the earth's surface. Even after the snow has melted completely, wet soil can maintain colder surface temperatures for longer periods of time.

(iv) Persistent snow anomalies can produce anomalous meridional temperature gradients and anomalous vertical wind shears. Snow is also a good insulator,

and in the presence of deep snow cover, nighttime inversions tend to be much stronger.

2.5 Sea Ice

Although sea ice fluctuations cover a very small fraction of the earth's surface, they can produce important changes in the atmospheric circulation over the polar regions, and for favorable dynamical structure of the large scale flow, these effects could also propagate to middle and subtropical latitudes. The local effect of sea ice anomalies is very large, because it directly changes the heat and moisture supply to the atmosphere. There have been several observational studies to determine possible relationships between sea ice extent and atmospheric circulation anomalies (for a review of these studies, see Walsh (1978), and Walsh and Johnson (1978, 1979)). In a numerical experiment conducted by Herman and Johnson (1979) using the GLAS climate model, it was found that the sea ice anomalies in the Arctic regions not only affected the local circulation but they also produced significant differences in middle and subtropical latitudes. More experimentation with simple models and realistic GCMs are needed to understand the sea ice effects. Since sea ice anomalies, like SST and snow, also change slowly compared to the atmospheric anomalies they can be prescribed from observations.

3. PREDICTABILITY OF THE TROPICAL ATMOSPHERE

The tropical atmosphere is potentially more predictable than the mid-latitudes because its planetary scale circulations are dominated by monsoon circulations which are intrinsically more stable than mid-latitude Rossby regime. Interaction of the large scale overturnings with the tropical disturbances (easterly waves, depressions, cyclones, etc.) is not strong enough to detract from the

predictability of the planetary scale circulations. Tropical disturbances are initiated by barotropic-baroclinic instabilities but their main energy source is the latent heat of condensation. Although their growth rate is fast and they are deterministically less predictable, their amplitude equilibration is also quite rapid and with the exception of hurricanes, they attain only moderate intensity. The intensity and geographical locations of the planetary scale circulations are primarily determined by the boundary conditions and not by synoptic scale disturbances. It is reasonable to assume that frequency and tracks of depressions and easterly waves are primarily determined by the location and intensity of the planetary scales and distribution of SST and soil moisture fields. It is highly unlikely that the synoptic scale tropical disturbances, through their interaction with planetary scale disturbances, will drastically alter the character of large scale tropical circulation. This is in marked contrast to the case of mid-latitudes where interaction between synoptic scale instabilities and planetary scale circulations is sufficiently strong so that baroclinically unstable disturbances can make the large scales unpredictable: the mid-latitude circulation consists of a continuum of scales whereas tropical circulation has a clear scale separation in terms of the frequency and the zonal wavenumber.

Charney and Shukla (1981) have suggested that since large scale monsoon circulation is stable with respect to dynamic instabilities, and since boundary conditions exert significant influence on the time averaged monsoon flow, the monsoon circulation is potentially more predictable than the middle latitude circulation. This suggestion was made by examining the variability among the monthly mean (July) circulation of four model runs for which the boundary conditions were kept identical, but the initial conditions were randomly perturbed. It was found that although the observed and the model variabilities

were comparible for middle and high latitudes, the variability among the four model runs for the monsoon region was far less than the observed interannual variability of the atmosphere as a whole. This led to the suggestion that part of the remaining variability could be due to the boundary forcings.

We have extended the work of Charney and Shukla (1981) and compared the model variability for climatological and observed SST anomalies. We have carried out 45 day integrations of the GLAS climate model for seven different sets of initial conditions and boundary conditions. In four of these integrations, the climatological global SST was used. In the remaining three, the observed SST for 1973, 1974 and 1975 was used between 0-30°N. Figure 9 shows the plots of zonally averaged values of standard deviations σ_p, σ_B and σ_o, and ratios σ_o/σ_p and σ_o/σ_B as a function of latitude. σ_p is the model standard deviation among predictability integrations (climatological SST and random perturbation in initial conditions), σ_B is the model standard deviation for SST anomalies, and σ_o is the standard deviation for 10 years of observations. It is seen that, in agreement with the results of Charney and Shukla, the ratio σ_o/σ_p is more than two in the tropics and close to one in the middle latitudes. The new result of this study is that σ_B (variability due to changes in SST boundary conditions) lies nearly halfway between σ_o and σ_p. This suggests that nearly half of the potentially predictable variability is accounted for by changes in SST between 0-30°N.

These conclusions are further supported by a more comprehensive study by Manabe and Hahn (1981), who integrated the GFDL spectral climate model for 15 years with prescribed but seasonally varying boundary conditions of SST. Figure 10a (reproduced from Manabe and Hahn (1981)) shows the values of zonally averaged standard deviation of 1000 mb geopotential height for a 15 year model run (σ_m) and observations (σ_o). We have calculated the ratio (σ_o/σ_m) from the

two curves of Manabe and Hahn and the ratio is also shown in Figure 10a. It is again seen that the ratio (σ_o/σ_m) is about two in the near equatorial regions and reduces to about one in the middle and high latitudes. Figure 10b (which is reproduced from Figure 5.10 of Manabe and Hahn) shows the latitude and height cross sections of interannual variability of geopotential height. It is seen that the ratio between the observed variability and the model variability is more than three in the tropical upper troposphere. It should be pointed out, however, that although SST was not varying from one year to the other for the 15 year model run, the soil moisture and snow cover were still variable during different years, and therefore, it is likely that part of the simulated model variability in the tropics, and perhaps even in the middle latitudes, could be due to the interannual variability of soil moisture and snow cover.

It is reasonable to conclude that although for short and medium range the tropical atmosphere is less predictable, the time averages (monthly and seasonal means) for the tropics have more potential predictability. Since there is sufficient evidence that tropical heat sources can also influence the middle latitude circulation, it is likely that, even for mid-latitudes, the monthly means could be potentially predictable due to their interaction with low latitudes.

4. POTENTIAL PREDICTABILITY OF MONTHLY MEANS AS DEDUCED FROM OBSERVATIONS

As pointed out in the Introduction, the interannual variability of monthly means is determined by complex interactions between the internal dynamics and surface boundary forcings. It is therefore difficult to determine their separate contributions by analysis of observed data. One possible approach is to carry out controlled numerical experiments described earlier, provided that all the boundary forcings can be reasonably prescribed.

Madden (1976) has examined the predictability of monthly mean sea level pressure over the Northern Hemisphere by comparing the variances of the observed monthly means with the natural variability of the monthly means. His study concluded that there are several areas over the Northern Hemisphere for which the ratio of the above two variances is more than one and therefore there is potential predictability. However, in Madden's study, the predictable signal was assumed to be only that part of the variance which is above white noise for more than 96 day time scales. He further assumed that the boundary forcings do not contribute to variability for time scales shorter than 96 days. Since it is well known that changes in boundary forcings can influence atmospheric fluctuations within 96 days, Madden's results should be considered only as the lower bound of the estimate of potential predictability of the monthly means of the atmospheric circulations (Shukla, 1983). Moreover, Madden's study does not address the question of dynamical prediction from an initial state.

Shukla and Gutzler (1983) have carried out an analysis of variance to compare the interannual variability of 500 mb geopotential height among 15 (1963-77) January months, and variability within each January. It can be hypothesized that if variability among the Januaries of different years is significantly larger than that due to the day to day variability within the individual Januaries, the excess variability could be due to boundary forcings. Since daily values within the individual Januaries are not independent of each other, we first calculated the time interval between independent samples which were used to calculate the effective sample size and effective degrees of freedom, and then calculated the natural variability of January means.

Figure 11a shows the ratio of the observed variability among the Januaries of different years and the natural variability. It is seen that the ratio between the two variances is larger than two (in some places, even larger than three) over a substantial part of the Northern Hemisphere. This suggests that

the boundary forcings play an important role in determining the interannual variability of monthly means. As mentioned earlier, these observational studies also suggest that for time averages (monthly and seasonal means) the tropical atmosphere is potentially more predictable than the mid-latitude atmosphere. This suggestion is further supported by a comparison of autocorrelation functions for the tropics and mid-latitudes. Figure 11b shows the zonally averaged values of autocorrelation calculated from 53 years (1925-77) of monthly mean sea level pressure data over the Northern Hemisphere analyzed by Trenberth and Paolino (1981). It is seen that the autocorrelation drops off much more sharply for mid-latitudes than in the tropics. The tropical spectra are redder than the mid-latitude spectra and therefore potentially more predictable.

5. CONCLUSIONS

We have briefly reviewed the physical mechanisms through which boundary forcings can influence the variability and predictability of monthly means. We have used a realistic global general circulation model to determine the sensitivity of the model circulation to changes in the boundary conditions of SST, soil moisture and surface albedo. From these studies it can be concluded that the slowly varying boundary forcings have the potential to increase the predictability of time averages. It is further suggested that correct specification of global boundary conditions of SST, soil moisture, surface albedo, sea ice, and snow is necessary for successful dynamical prediction of monthly means.

Anomalies of slowly varying boundary forcings produce anomalous sources of heat and moisture which in turn produce significant anomalies of atmospheric circulation. These effects can be either local in the vicinity of the boundary anomaly or away from the source if the intervening environment is favorable for the propagation of local influences. For example, tropical heat sources can produce significant changes in the extra-tropical circulation.

It should be pointed out that the anomalies of SST or soil moisture are neither necessary nor sufficient to produce changes in the mid-latitude circulation. For example, a warm SST anomaly in tropics can produce a local heat source, but if it occurs within the band of easterlies, its influence cannot propagate beyond the zero wind line. Conversely, even in the absence of SST and soil moisture anomalies, internal dynamics can produce persistent anomalies of precipitation and diabatic heating in the tropics which, under favorable zonal flow, can affect the mid-latitudes.

The main purpose of the two papers (Shukla (1981) and this paper) was to examine and establish a physical basis for dynamical prediction of monthly means. The essential reqiurements for establishing such a basis are to show that: a) fluctuations of monthly means are larger than can be expected due to sampling of day-to-day weather changes; b) there are low frequency planetary scale components of the circulation which remain predictable beyond the limits of synoptic scale predictability; and, c) influences of the slowly varying boundary conditions of SST, soil moisture, snow, sea ice, etc., are large enough to produce significant and detectable changes in the monthly mean circulations. In these two papers we have presented observational and numerical evidence which support the above requirements.

It is hoped that an accurate description of global boundary forcings can be obtained on a near-real time basis so that feasibility of experimental prediction of monthly means can be investigated using dynamical models.

ACKNOWLEDGEMENTS

We are grateful to Yale Mintz and Mike Wallace for reading the manuscript and making many valuable suggestions. We thank Miss Debbie Boyer for typing the manuscript and Miss Laura Rumburg for drafting the figures.

REFERENCES

Baumgartner, H., and E. Reichel, 1975: The world water balance: Mean annual global continental and maritime precipitation, evaporation and runoff. (Elsevier, Amsterdam/Oxford/New York, 179 pp and plates.)

Blanford, H. F., 1884: On the connection of the Himalaya snowfall with dry winds and seasons of droughts in India. Proc. Roy. Soc., London, 37, p. 3.

Charney, J. G., W. J. Quirk, S. Chow, and J. Kornfield, 1977: A comparative study of the effects of albedo change on drought in semi-arid regions. J. Atmos. Sci., 34, 1366.

Charney, J. G., and J. Shukla, 1981: Predictability of monsoons. Monsoon Dynamics, Cambridge University Press, Editors: Sir James Lighthill and R. P. Pearce.

Chen, T. C., and J. Shukla, 1983: Diagnostic analysis and spectral energetics of a blocking event in the GLAS climate model simulation. Mon. Wea. Rev., 111, 3-22.

Hahn, D., and J. Shukla, 1976: An apparent relationship between Eurasian snow cover and Indian monsoon rainfall. J. Atmos. Sci., 33, 2461-2463.

Herman, G. F., and W. T. Johnson, 1979: The sensitivity of the general circulation to Arctic Sea ice boundaries: A numerical experiment. Mon. Wea. Rev., 106, 1649-1664.

Horel, J. D., and J. M. Wallace, 1981: Planetary-scale atmospheric phenomena associated with the Southern Oscillation. Mon. Wea. Rev., 109, 813-829.

Hoskins, B. J., and D. J. Karoly, 1981: The steady linear response of a spherical atmosphere to thermal and orographic forcing. J. Atmos. Sci., 38, 1179-1196.

Lambert, S. J., and P. E. Merilees, 1978: A study of planetary wave errors in a spectral numerical weather prediction model. Atmos. Ocean, 16, 197-211.

Madden, R. A., 1976: Estimates of the natural variability of time-averaged sea-level pressure. Mon. Wea. Rev., 104, 942-952.

Manabe, S., and D. G. Hahn, 1981: Simulation of atmospheric variability. To be published in Mon. Wea. Rev.

Mintz, Y., 1982: The sensitivity of numerically simulated climates to land-surface boundary conditions. NASA Tech. Memo. 83985, 81 pp.

Moura, A. D., and J. Shukla, 1981: On the dynamics of droughts in northeast Brazil: Observations, theory and numerical experiments with a General atmospheric behavior, Proceedings of the International Symposium on Numer-

Namias, J., 1962: Influence of abnormal surface heat sources and sinks on atmospheric behavior. Proceedings of the International Symposium on Numerical Weather Prediction, pp. 615-629, Meteorol. Soc. of Japan, Tokyo.

Namias, J., 1978: Multiple causes of the North American abnormal winter 1967-77. Mon. Wea. Rev., 106, 279-295.

Rasmusson, E., and T. Carpenter, 1982: Variations in tropical sea surface temperature and surface wind fields associated with the Southern Oscillation/El Nino. Mon. Wea. Rev., 110, 354-384.

Shukla, J., 1975: Effect of Arabian sea-surface temperature anomaly on Indian summer monsoon: A numerical experiment with the GFDL model. J. Atmos. Sci., 32, 503-511.

Shukla, J., and B. Bangaru, 1979: Effect of a Pacific sea surface temperature anomaly on the circulation over North America. GARP Publication Series No. 22, 501-518.

Shukla, J., 1981: Dynamical predictability of monthly means. J. Atmos. Sci., 38, 2547-2572.

Shukla, J., 1983: Comments on natural variability and predictability. Mon. Wea. Rev., 111.

Shukla, J., and D. S. Gutzler, 1983: Interannual variability and predictability of 500 mb geopotential heights over the Northern Hemisphere. Mon. Wea. Rev., 111.

Shukla, J., and R. Lindzen, 1981: Stationary waves and deterministic predictability. Presented at the Third Conference on Atmospheric and Oceanic Waves and Stability, January 19-23, 1981, San Diego, California.

Shukla, J., and Y. Mintz, 1982: The influence of land-surface evapotranspiration on the earth's climate. Science, 214, 1498-1501.

Shukla, J., and J. M. Wallace, 1983: Numerical simulation of the atmospheric response to equatorial Pacific sea surface temperature anomalies. J. Atmos. Sci., 40.

Sud, Y., and M. Fennessy, 1982: A numerical simulation study of the influence of surface-albedo on July circulation in semi-arid regions using the GLAS GCM. J. of Climatology, 2, 105-125.

Trenberth K. E., and D. A. Paolino, 1981: Characteristic patterns of variability of sea-level pressure in the Northern Hemisphere. Mon. Wea. Rev., 109, 1169-1189.

Walker, G. R., 1910: Correlations in seasonal variations of weather II. Mem. Indian Meteor. Dept., 21, 22-45

Walsh, J. E., 1978: Temporal and spatial scales of the Arctic circulation. Mon. Wea. Rev., 106, 1532-1544.

Walsh, J. E., and C. M. Johnson, 1979: An analysis of Arctic Sea ice fluctuations, 1953-77. J. Phys. Oceanogr., 9, 580-591.

Walsh, J. E., and C. M. Johnson, 1979: Interannual atmospheric variability and associated fluctuations in Arctic Sea ice extent. J. Geophys. Res., 84, 6915-6928.

Washington, W. M., R. M. Chervin, and G. V. Rao, 1977: Effects of a variety of Indian Ocean surface temperature anomaly patterns on the summer monsoon circulation: Experiments with the NCAR General Circulation Mode. Pageoph, 115, 1335-1356.

Webster, P. J., 1981: Mechanisms determining the atmospheric response to sea surface temperature anomalies. J. Atmos. Sci., 38, 554-571.

Wiesnet, D. R., and M. Matson, 1976: A possible forecasting technique for winter snow cover in the Northern Hemisphere and Eurasia. Mon. Wea. Rev., 104, 828-835.

Yeh, T.-C., X.-S. Chen, and C.-B. Fu, 1981: The time-lag feedback processes of large-scale precipitation on the atmospheric circulation and climate--the air-land interaction. (pre-published manuscript)

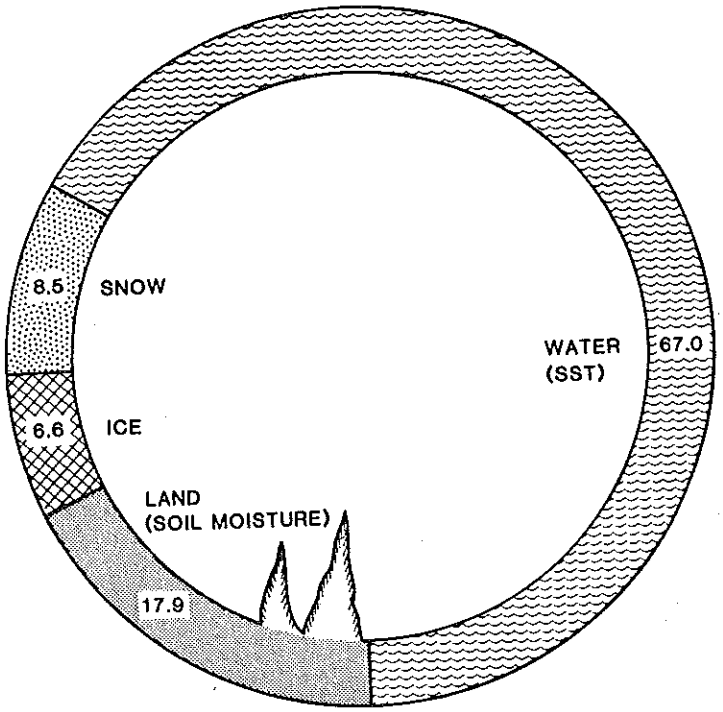

Figure 1a. Schematic representation of the atmosphere's lower boundary. Numbers denote the percentage of earth surface area covered by different boundary forcings during January.

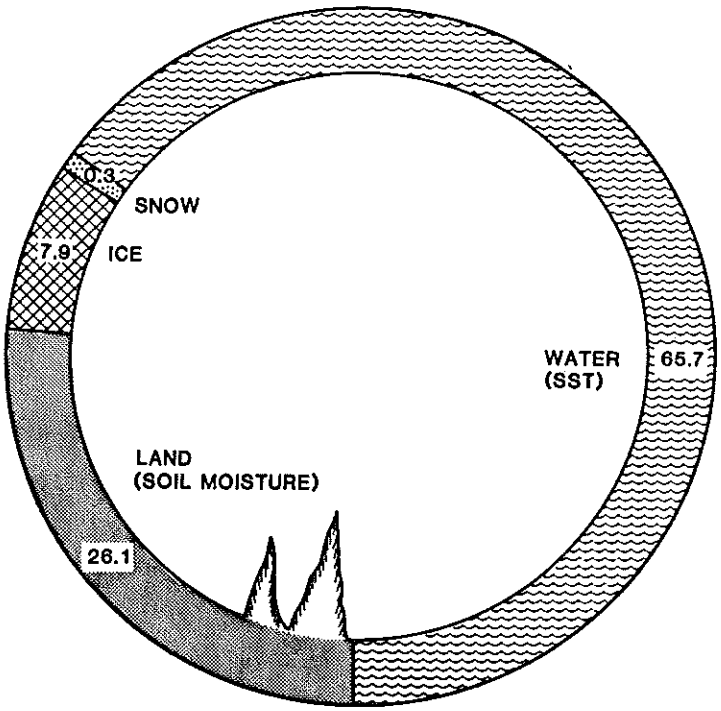

Figure 1b. Schematic representation of the atmosphere's lower boundary. Numbers denote the percentage of earth surface area covered by different boundary forcings during July.

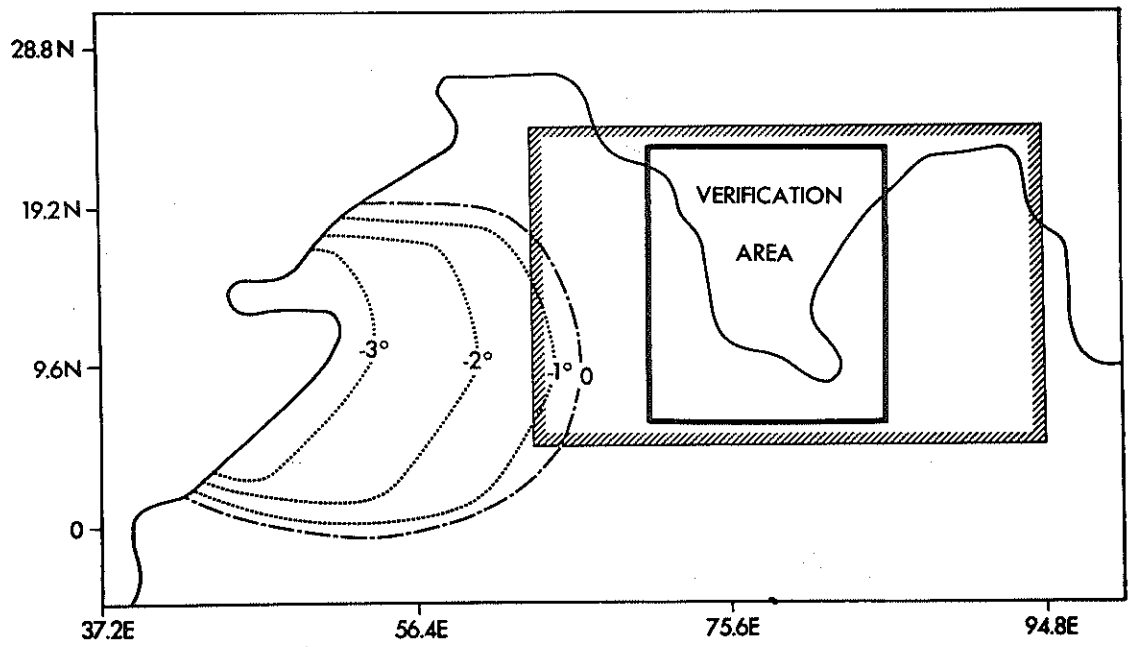

Figure 2a. Sea surface temperature anomaly (°C) over the Arabian Sea used for the GCM experiment and the area of verification.

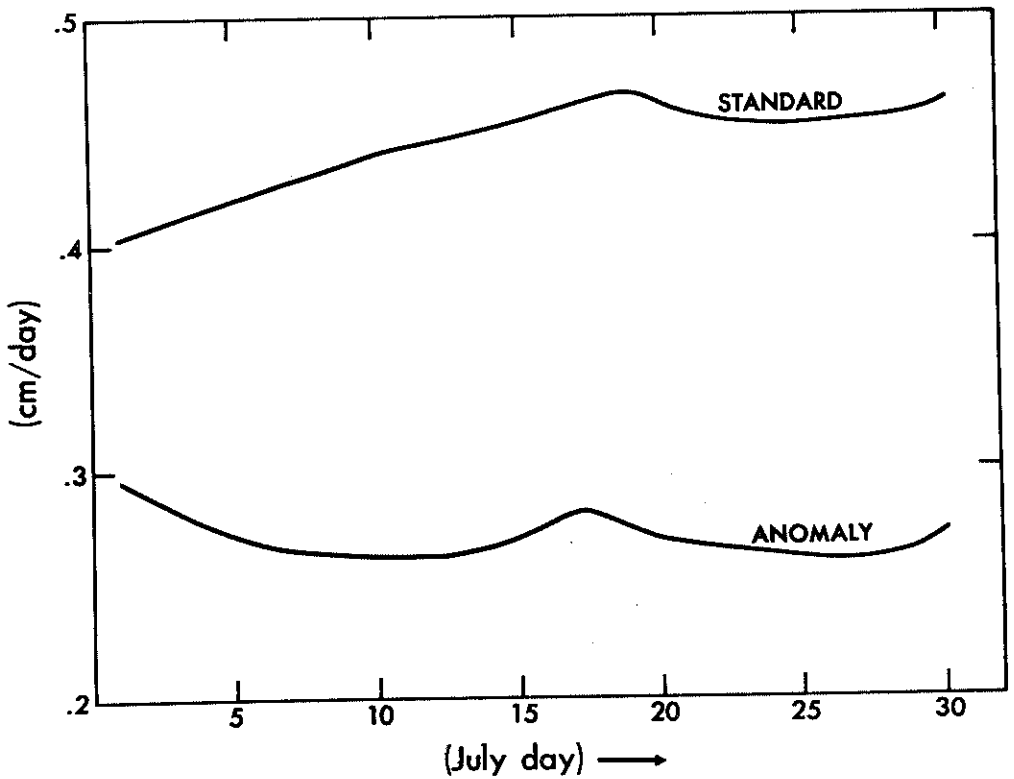

Figure 2b. 15 day running mean of the rate of precipitation (cm day^{-1}) averaged over the verification area for the standard and anomaly runs.

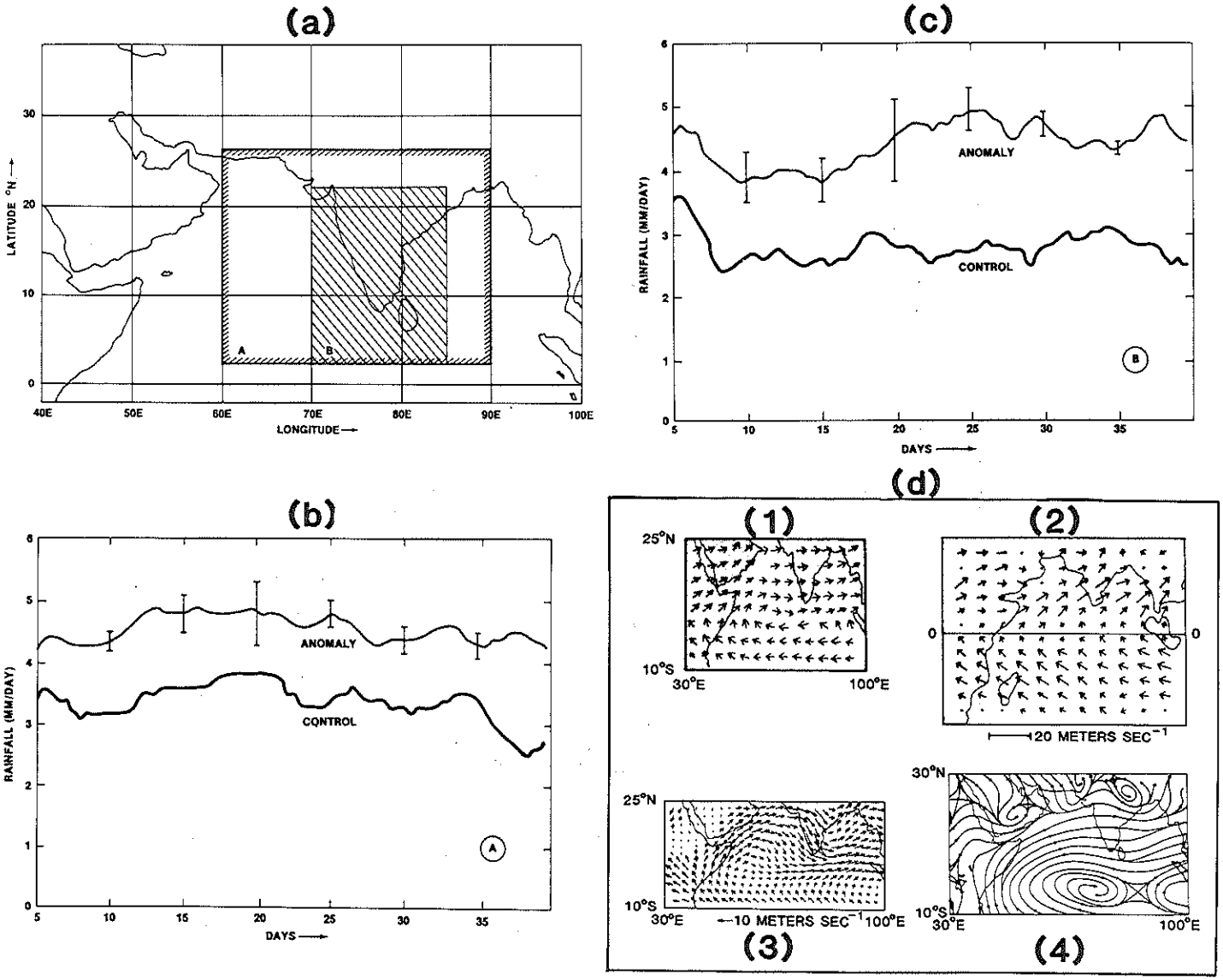

Figure 3. Panels (b) and (c) show the daily values of rainfall for control and anomaly runs averaged over areas A and B shown in panel (a). Length of the error bars represent standard deviation among three anomaly runs. Panel (d) shows the low level wind field for: (1) GLAS model, (2) GFDL model, (3) NCAR model, and (4) Observations.

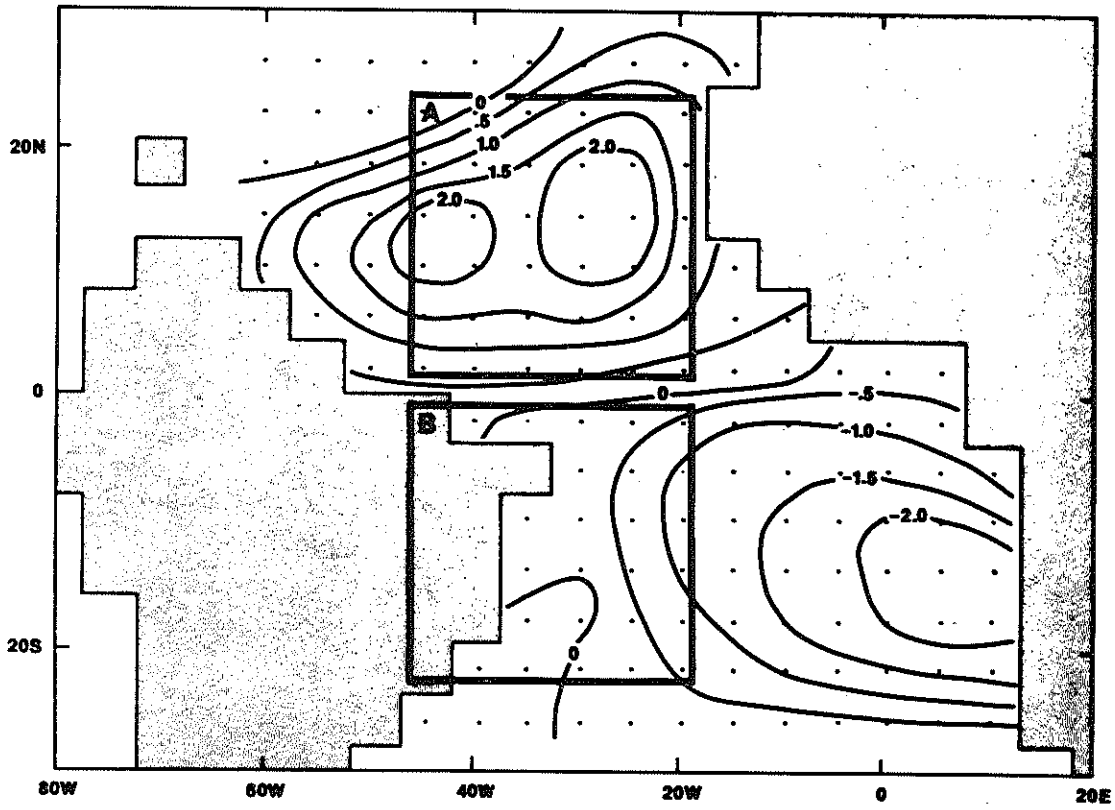

Figure 4a. Sea surface temperature anomaly (°C) over the tropical Atlantic used for the GCM experiment.

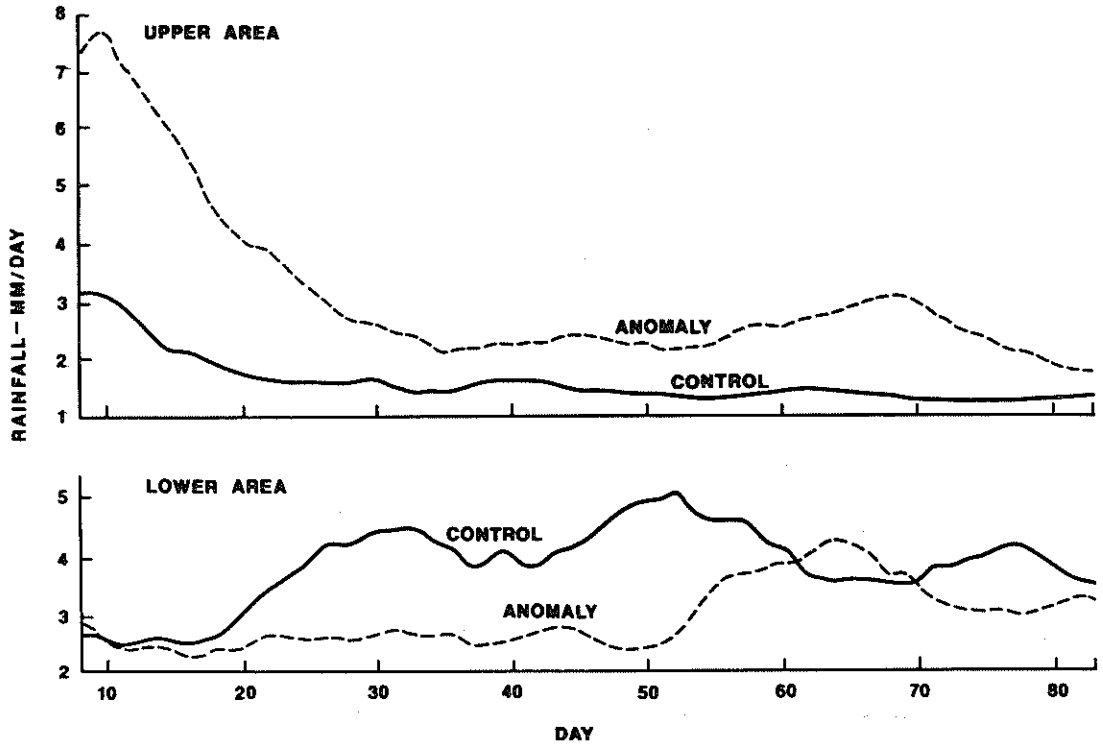

Figure 4b. 15 day running mean of daily rainfall (mm/day) for upper area (A) and lower area (B). (From Moura and Shukla, 1981).

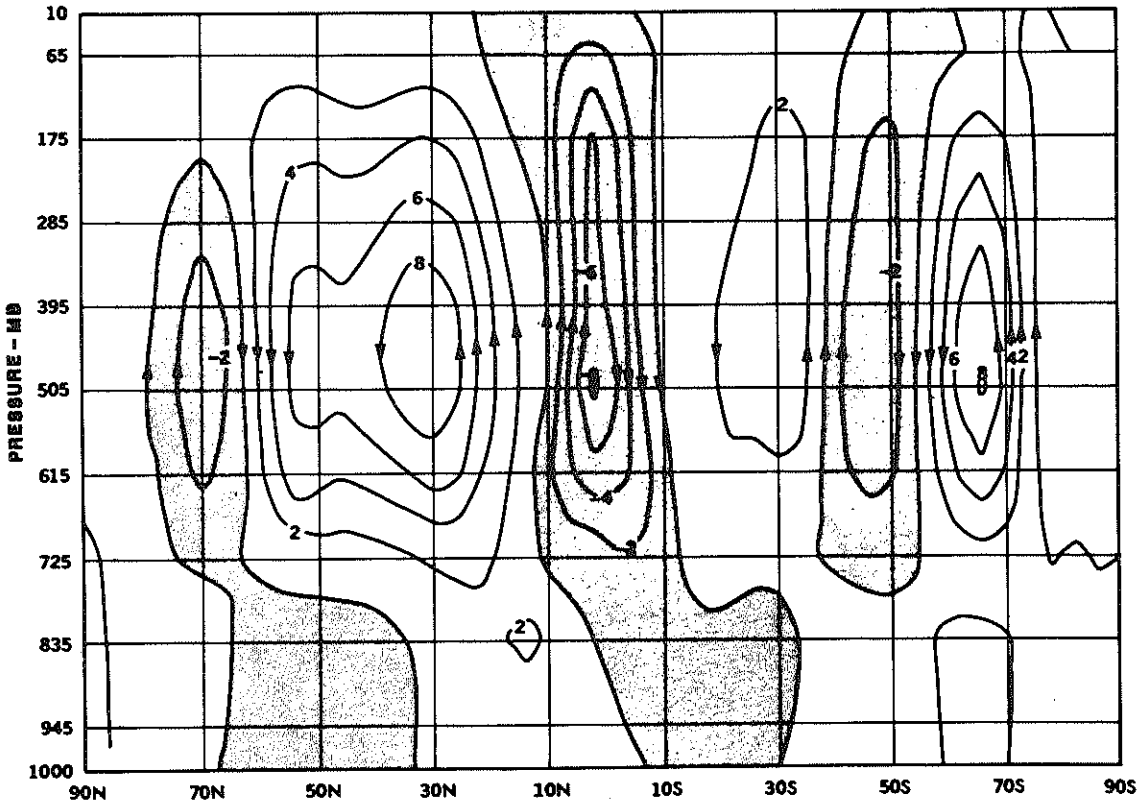

Figure 4c. Difference of 60 day mean meridional circulation (10^{13}gm/sec) averaged between the longitudes 50°W and 5°W. (From Moura and Shukla, 1981).

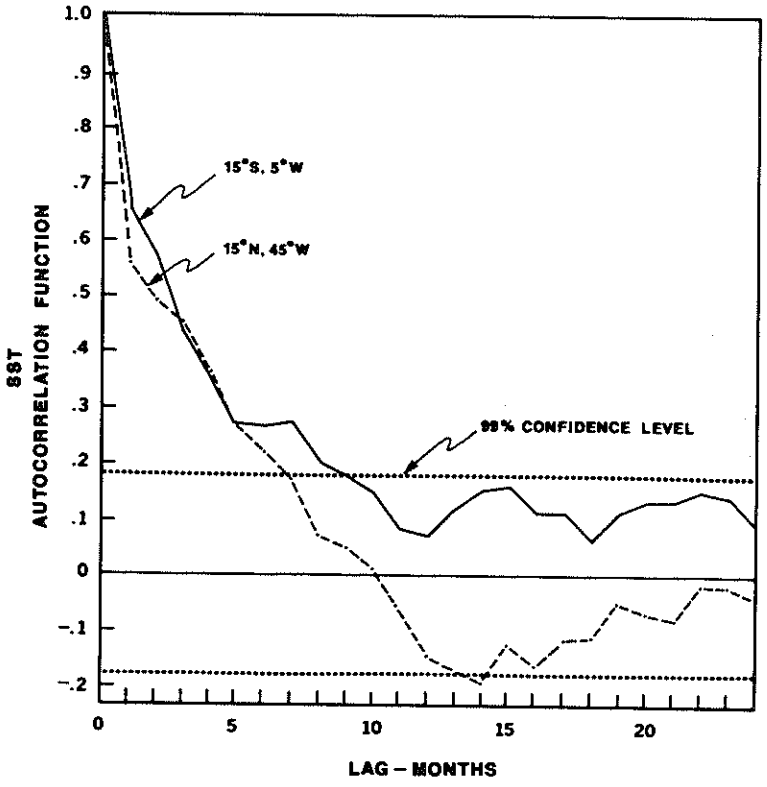

Figure 4d. Lag correlation function for monthly mean SST anomaly at 15°S, 5°W and 15°N, 45°W. (From Moura and Shukla, 1981)

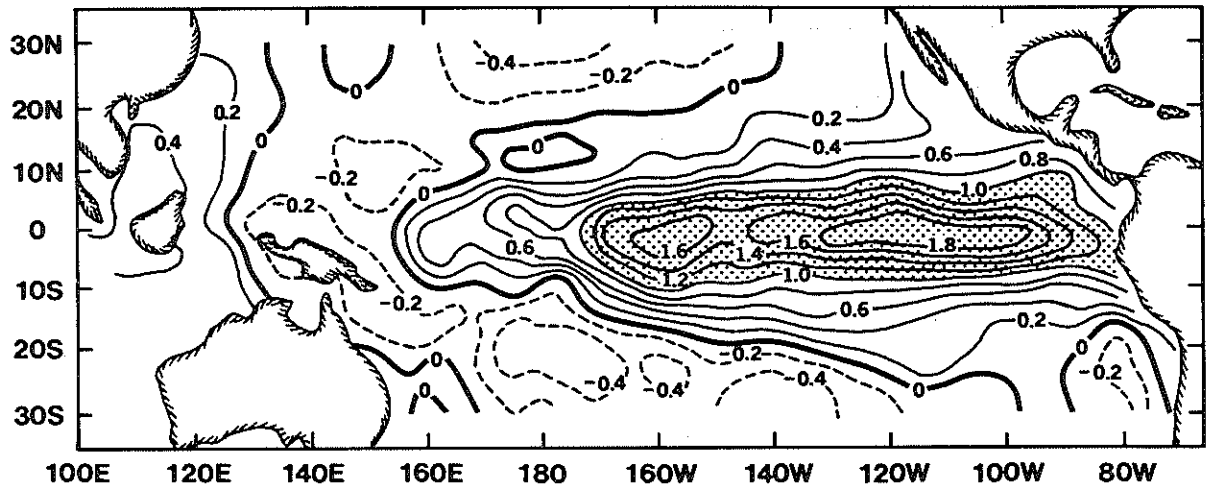

Figure 5a. Sea surface temperature anomaly (°C) used for the GCM experiment.

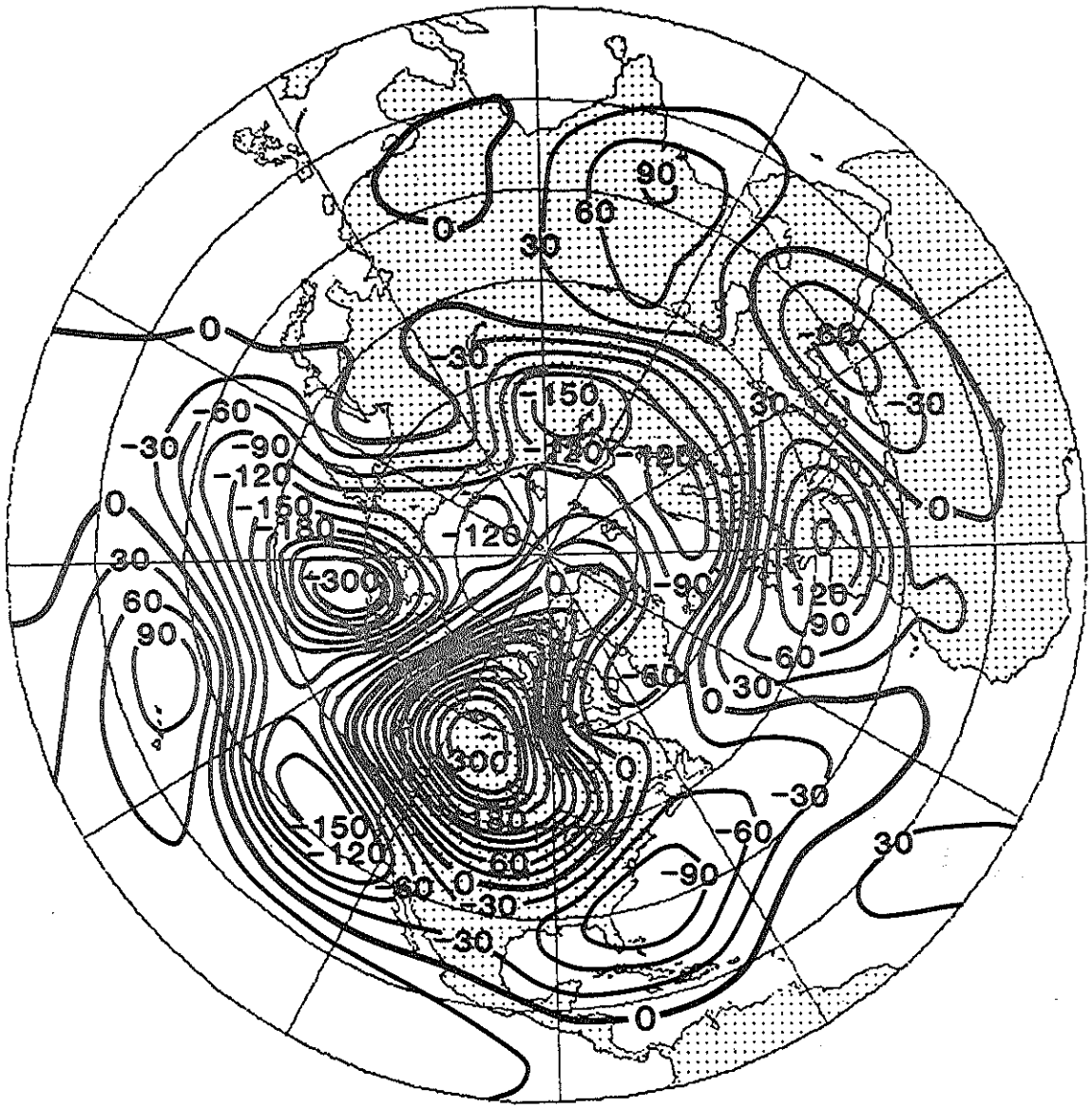

Figure 5b. Difference (anomaly-control) of 300 mb geopotential height field averaged for days 11-25.

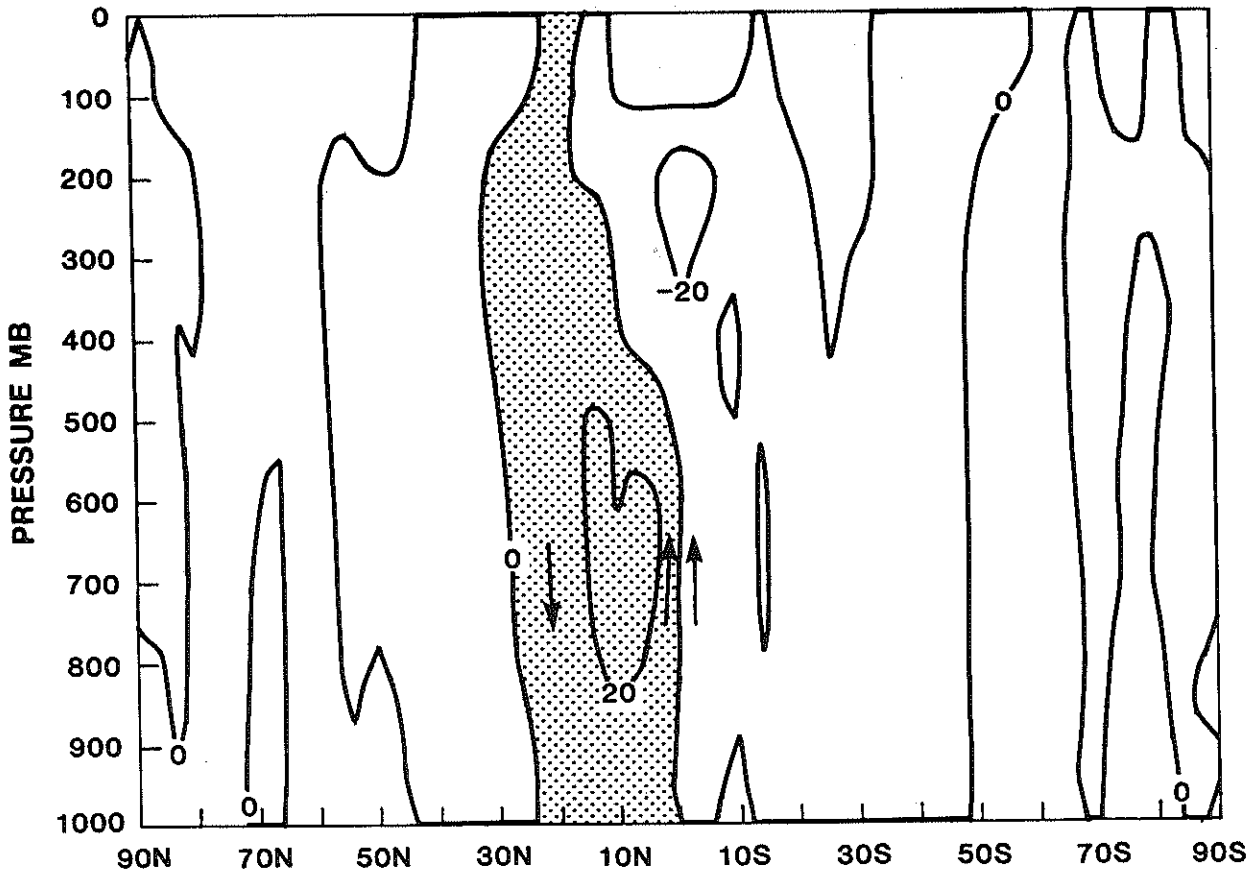

Figure 5c. Difference (anomaly-control) of Hadley cell (in units of 10^9 kg/sec) averaged for days 6-25.

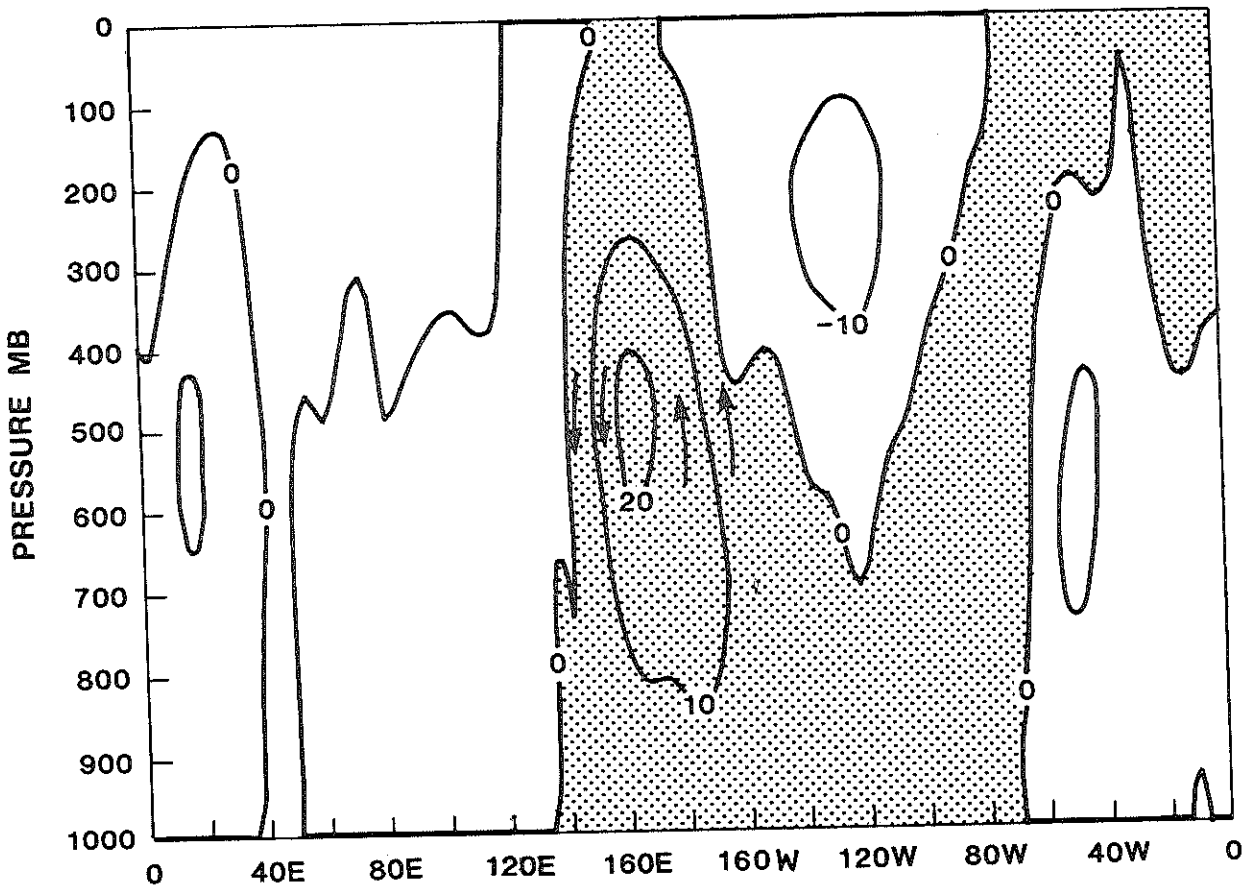

Figure 5d. Difference (anomaly-control) of Walker cell (in units of 10^9 kg/sec) averaged between 6°N-6°S and averaged for days 6-25.

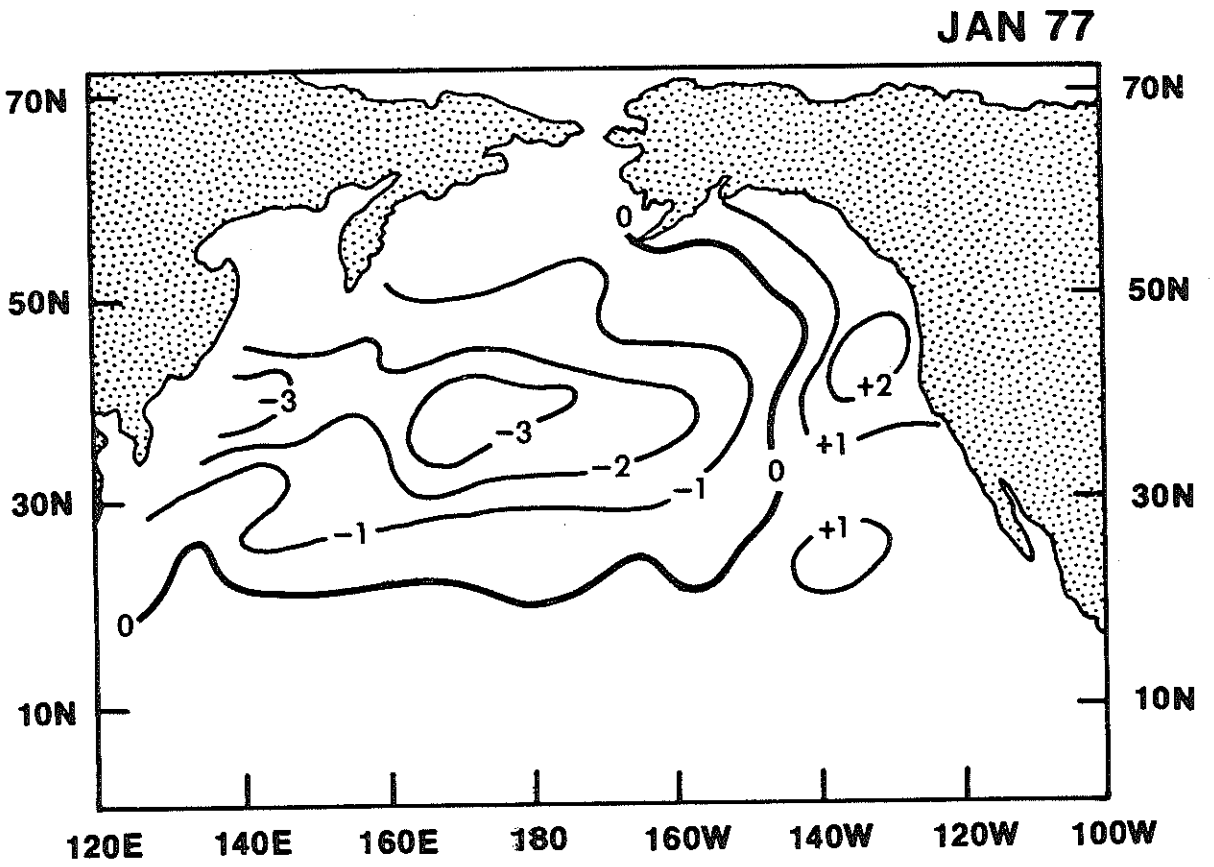

Figure 6a. Sea surface temperature anomaly (°C) over the north Pacific used for the GCM experiment. This anomaly pattern will be identical to the observed SST anomaly during January 1977 if the units are changed from (°C) to (°F).

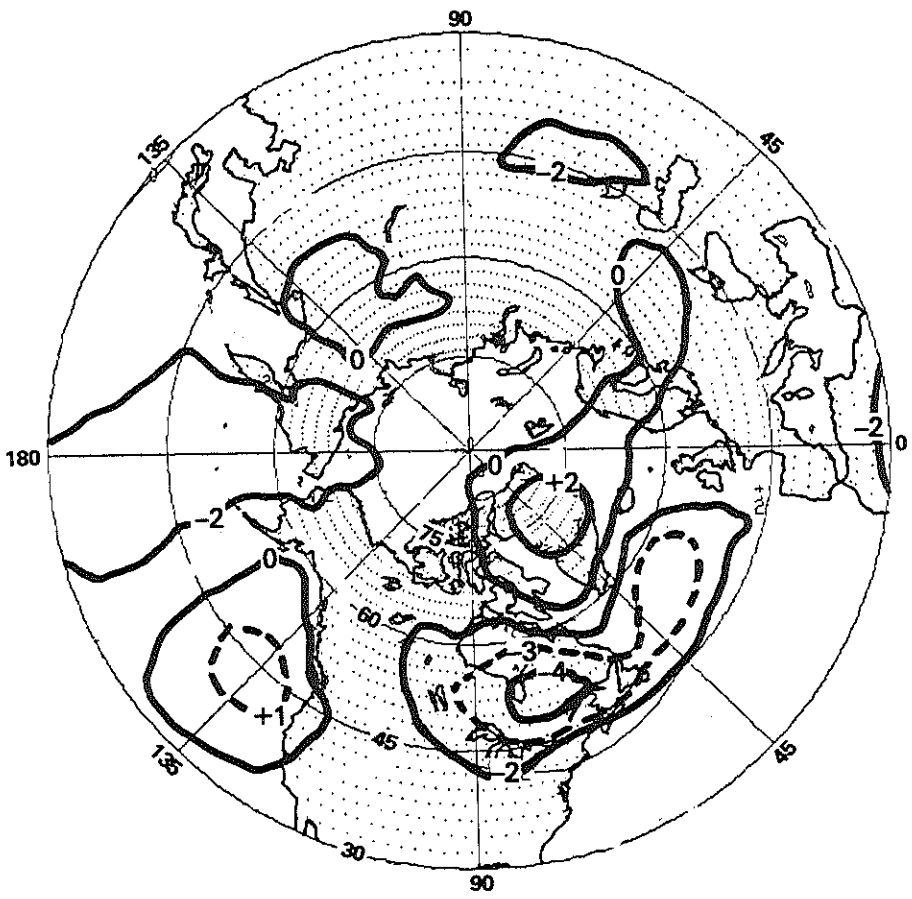

Figure 6b. Temperature difference (°C) at 700 mb between the average of the two anomaly runs and the average of the six control runs, averaged for days 15-45.

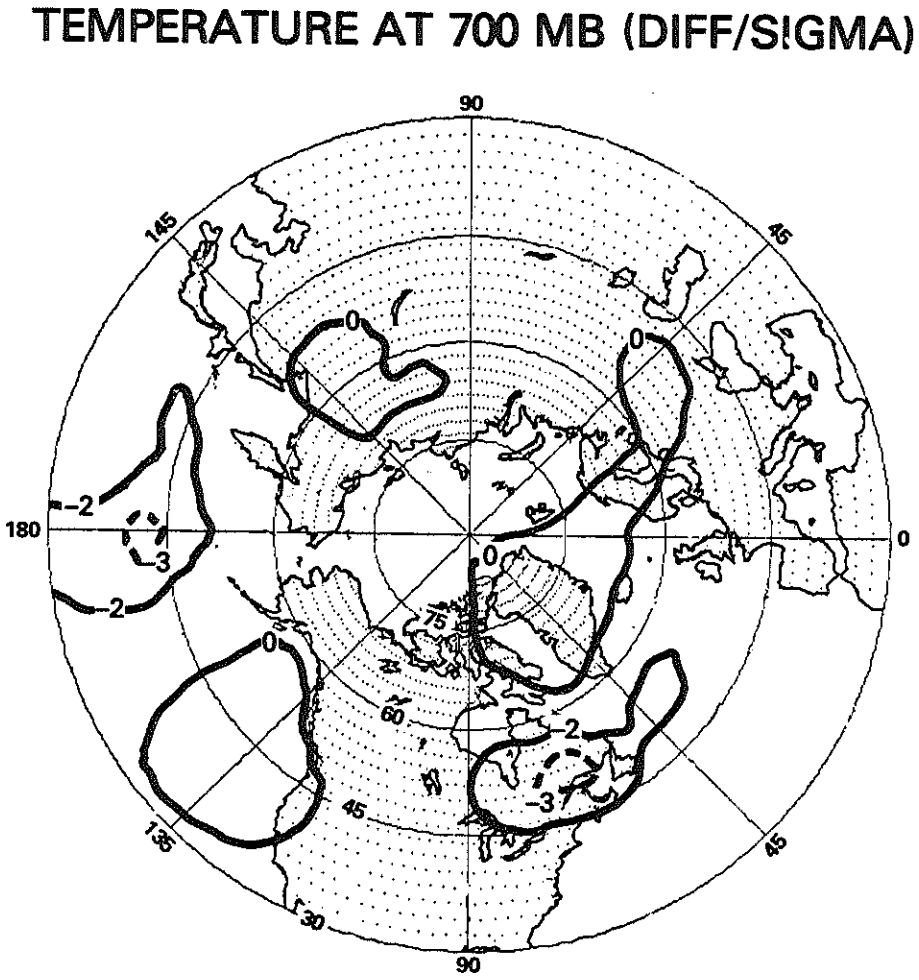

Figure 6c. Ratio of the temperature difference at 700 mb (shown in Figure 6b) to the standard deviation among 15-45 day averages of six control runs.

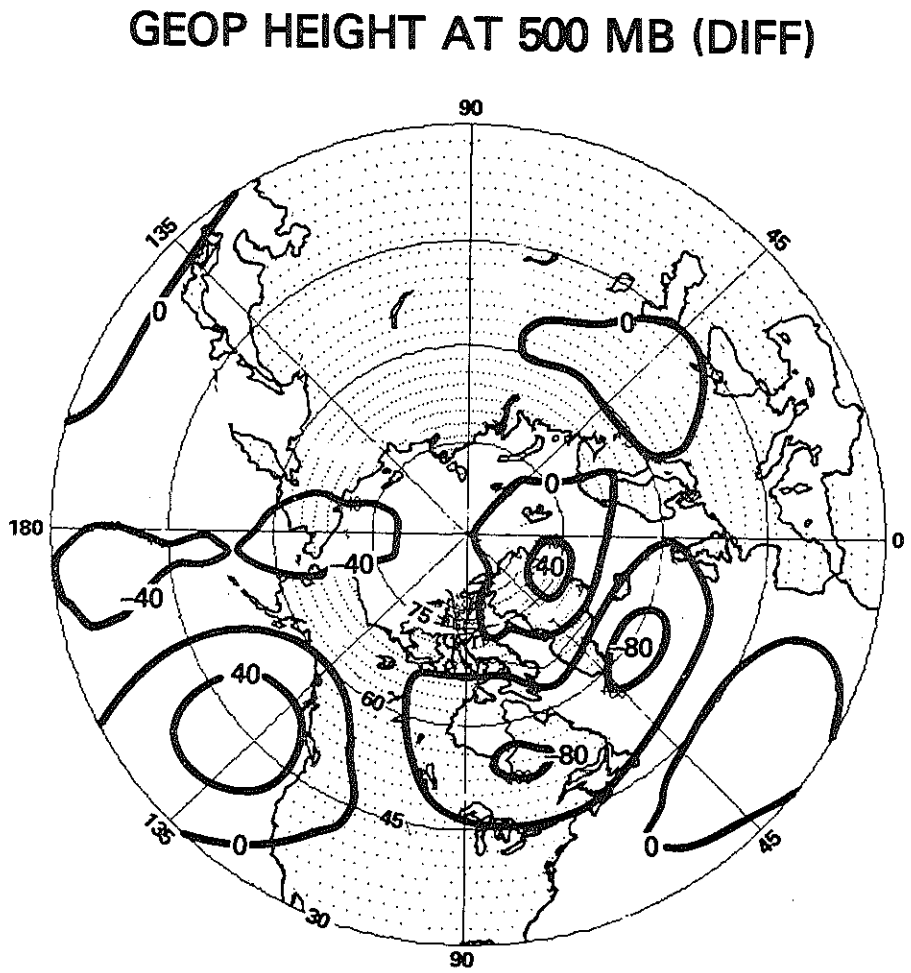

Figure 6d. Geopotential height difference (meters) at 500 mb between the average of two anomaly runs and the average of the six control runs averaged for days 15-45.

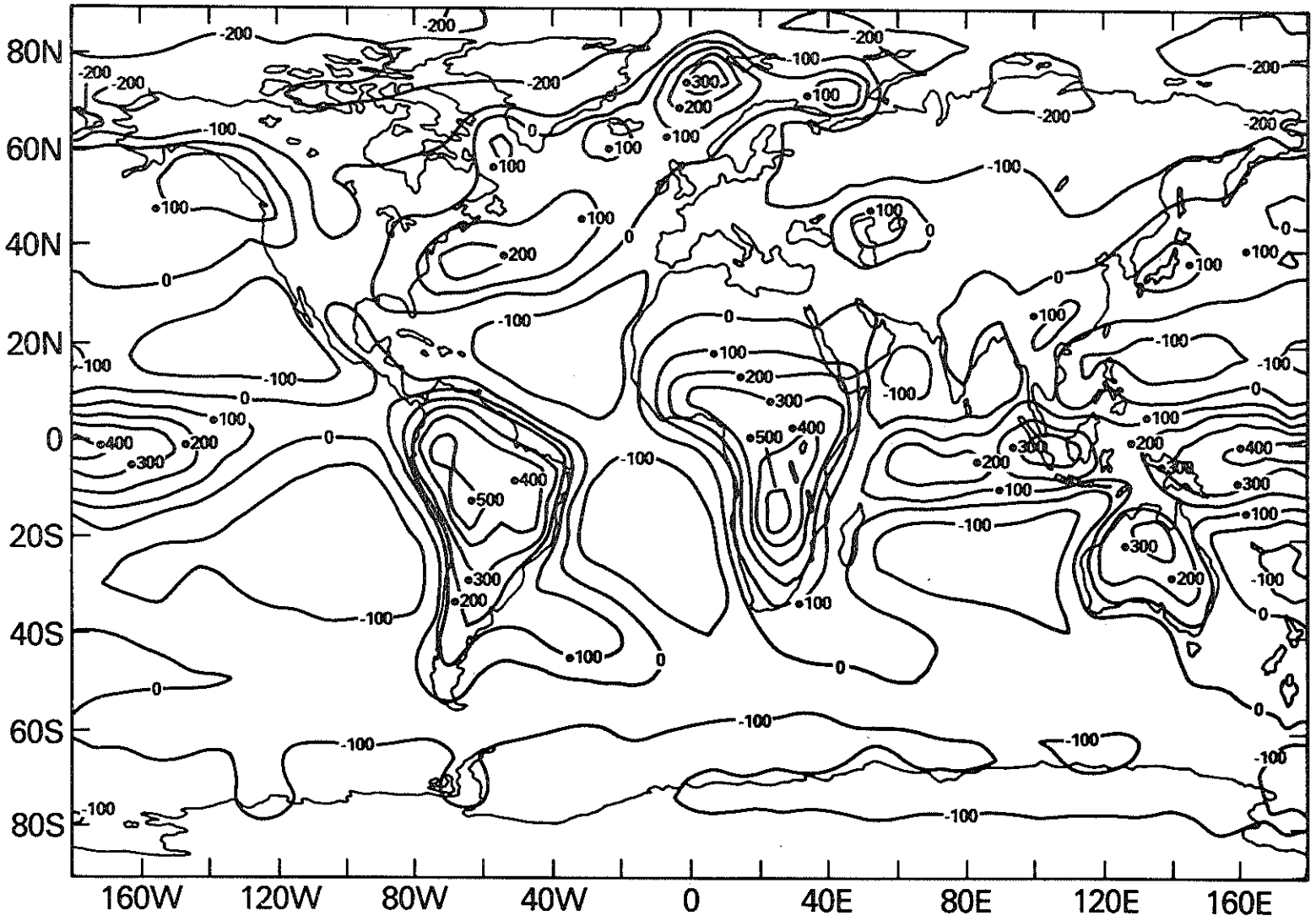

Figure 7a. Vertically integrated net diabatic heating (cal cm^{-2} day^{-1}) of the atmosphere during winter, as simulated by the GLAS climate model.

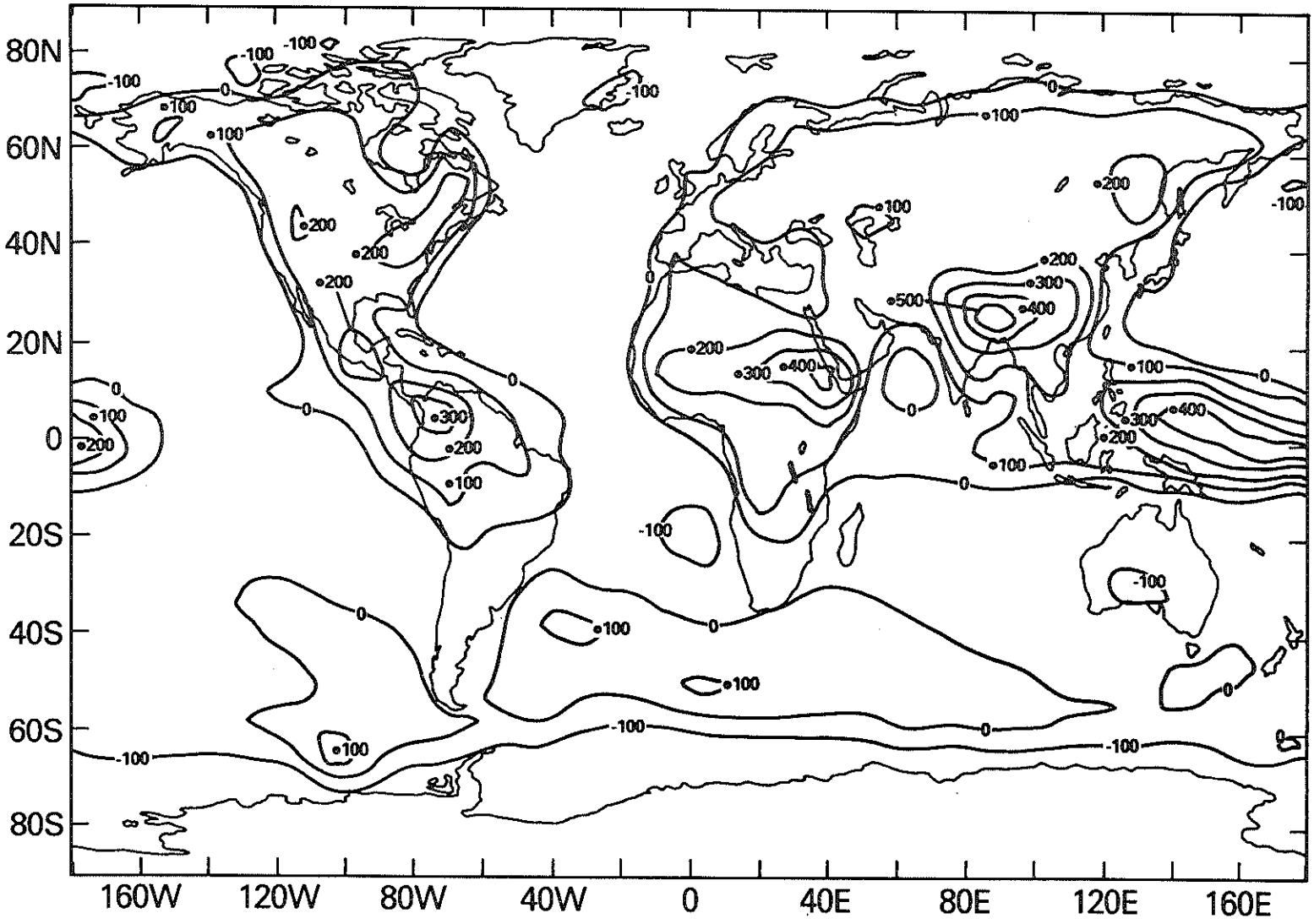

Figure 7b. Vertically integrated net diabatic heating (cal cm^{-2} day^{-1}) of the atmosphere during summer, as simulated by the GLAS climate model.

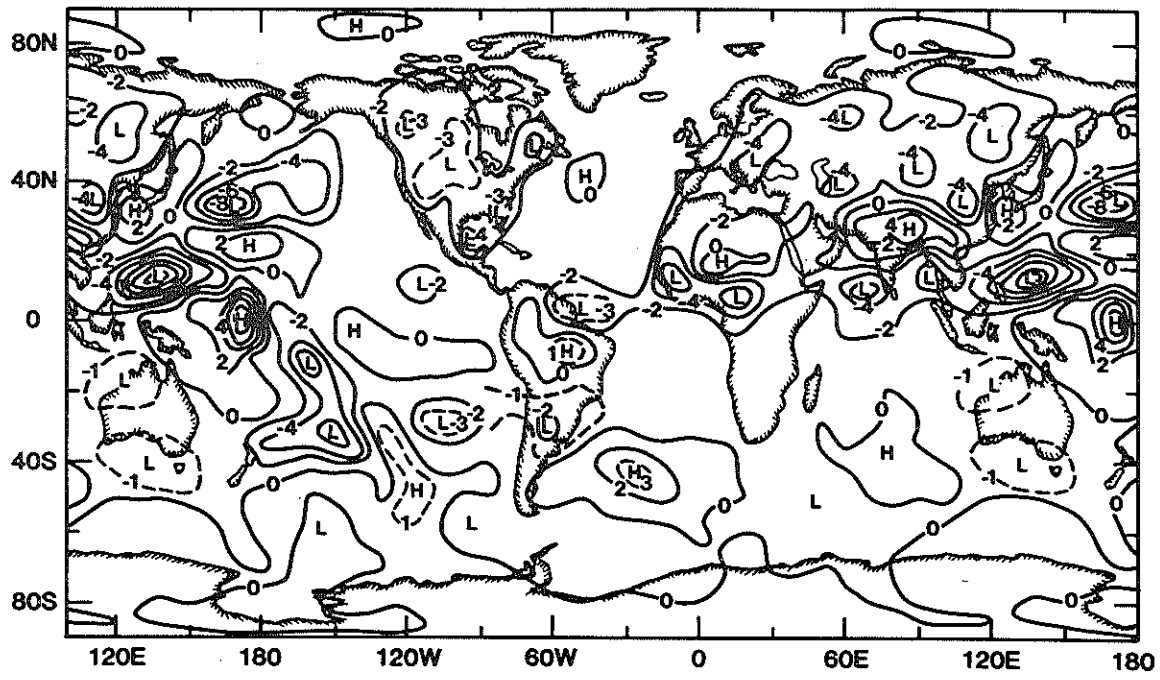

Figure 7c. Rainfall difference (mm/day) between two model simulations (dry soil-wet soil) for the month of July.

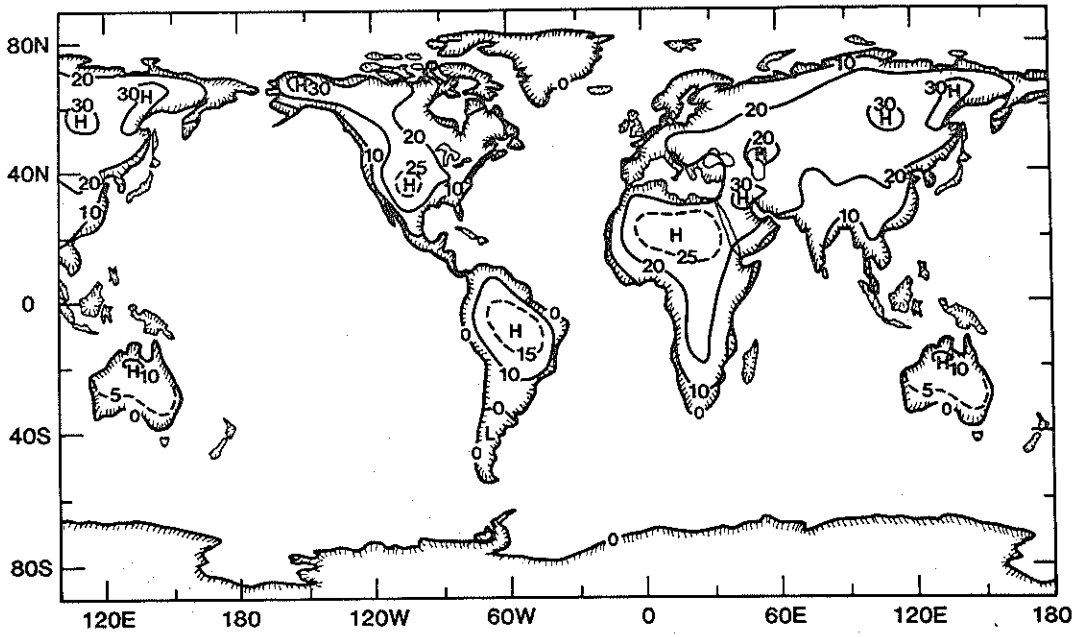

Figure 7d. Ground temperature difference (°C) between two model simulations (dry soil-wet soil) for the month of July.

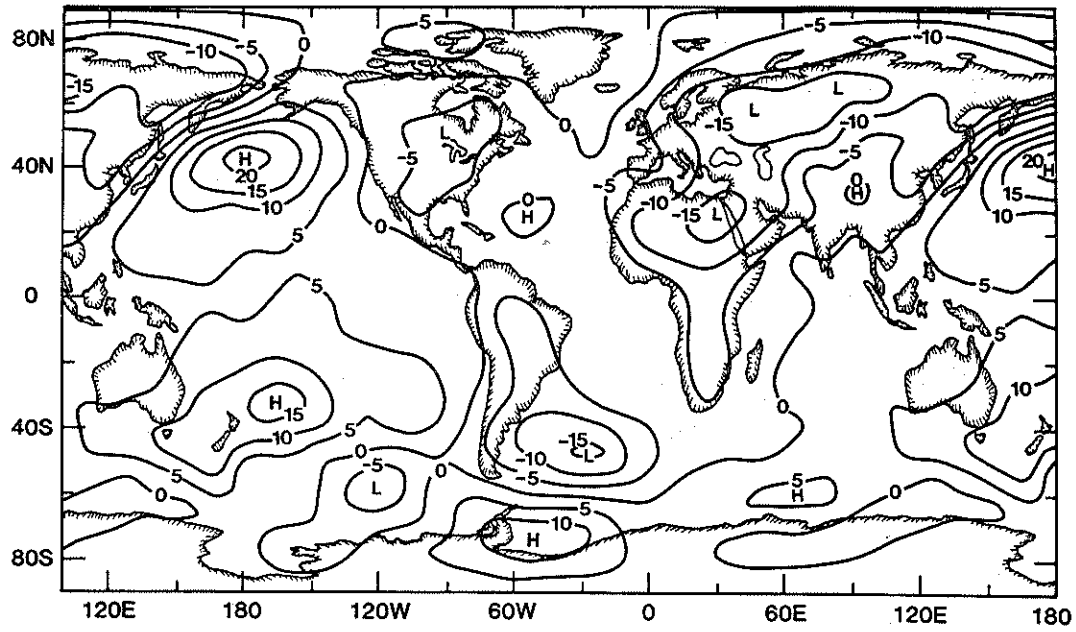

Figure 7e. Surface pressure difference (mb) between two model simulations (dry soil-wet soil) for the month of July.

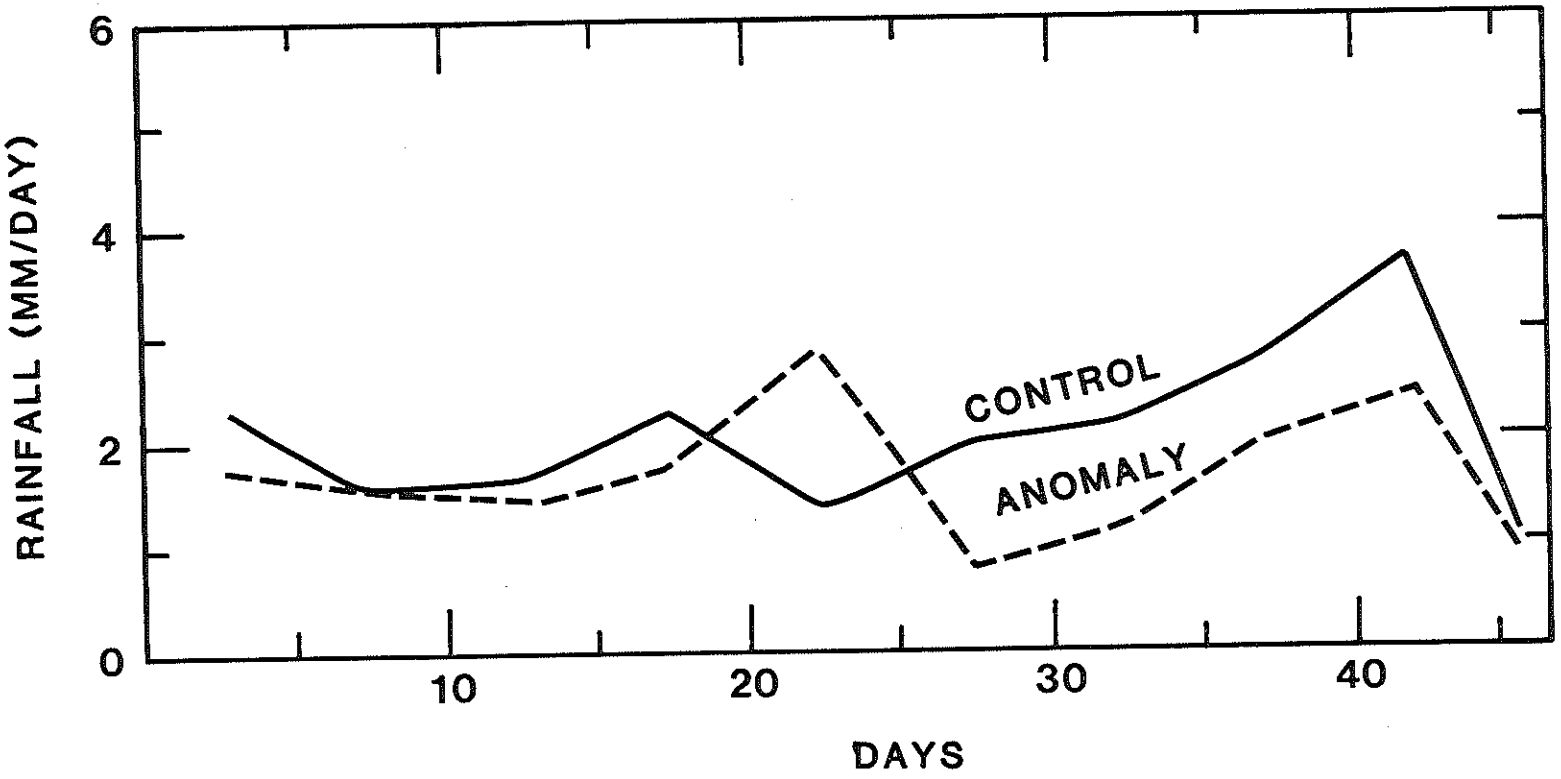

Figure 7f. Five day average rainfall over northeast Brazil, for control and anomaly run.

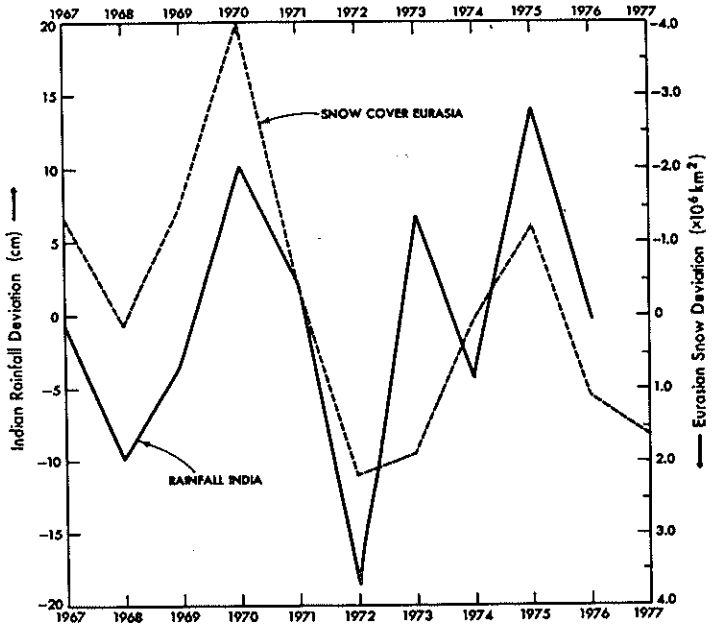

Figure 8. Area weighted average of percentage departure from normal summer monsoon rainfall over Indian subdivisions (solid line) and the preceding winter snow cover departure over Eurasia south of 52°N.

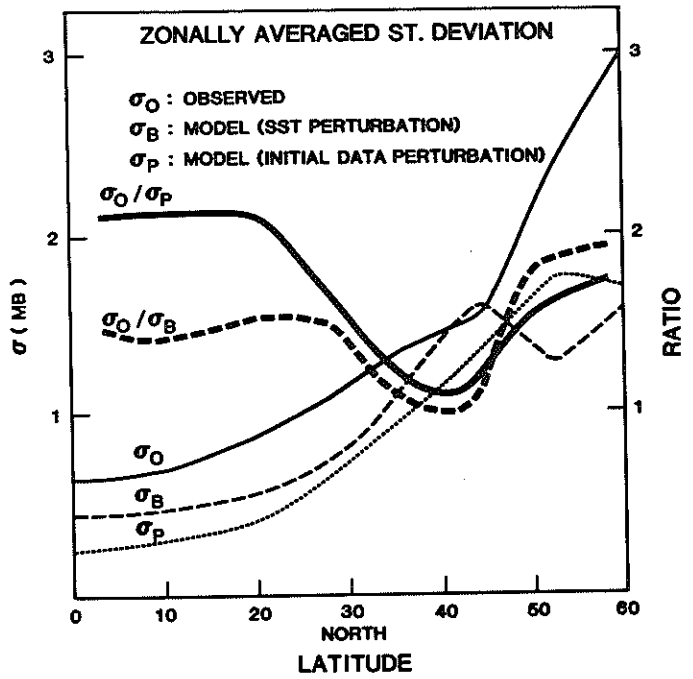

Figure 9. Zonally averaged standard deviation among monthly mean (July) sea level pressure (mb) for 10 years of observations (σ_O, thin solid line); four model runs with variable boundary conditions (σ_B, thin dashed line); and four model runs with identical boundary conditions (σ_p, thin dotted line). Thick solid line and thick dashed line show the ratio σ_O/σ_p and σ_O/σ_B respectively.

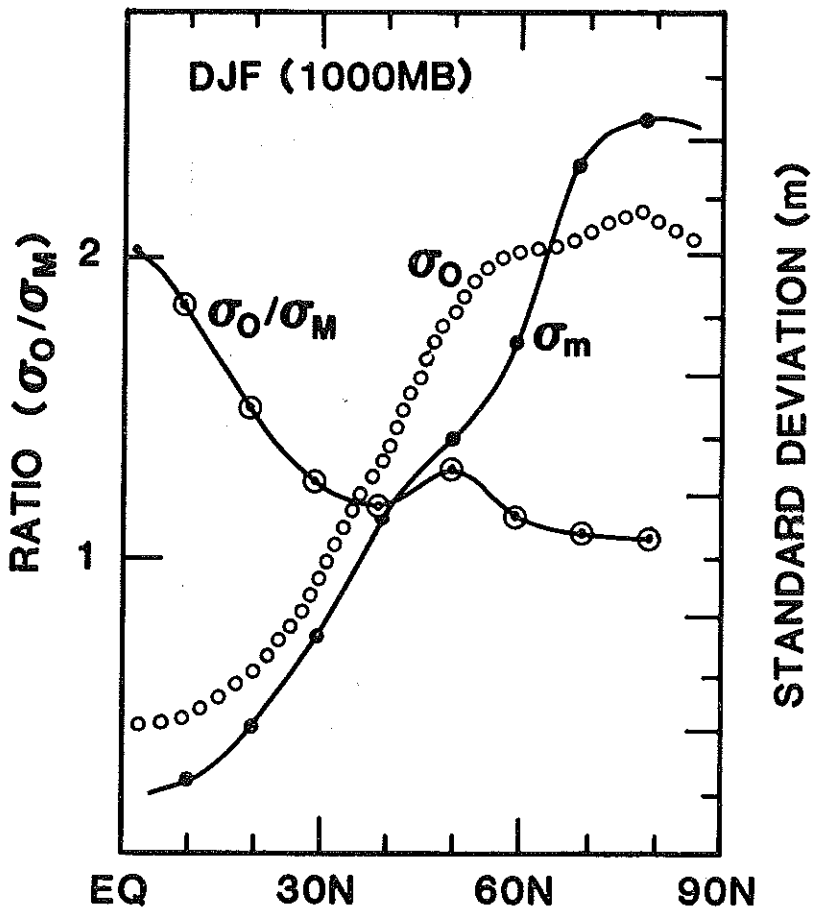

Figure 10a. Zonal means of standard deviation of monthly mean 1000 mb geopotential height (m) for the Dec.-Jan.-Feb. season. Observed distributions are from Oort and Jenne. The ratio of observed and model standard deviation is on the left hand side. (from Manabe and Hahn, 1981)

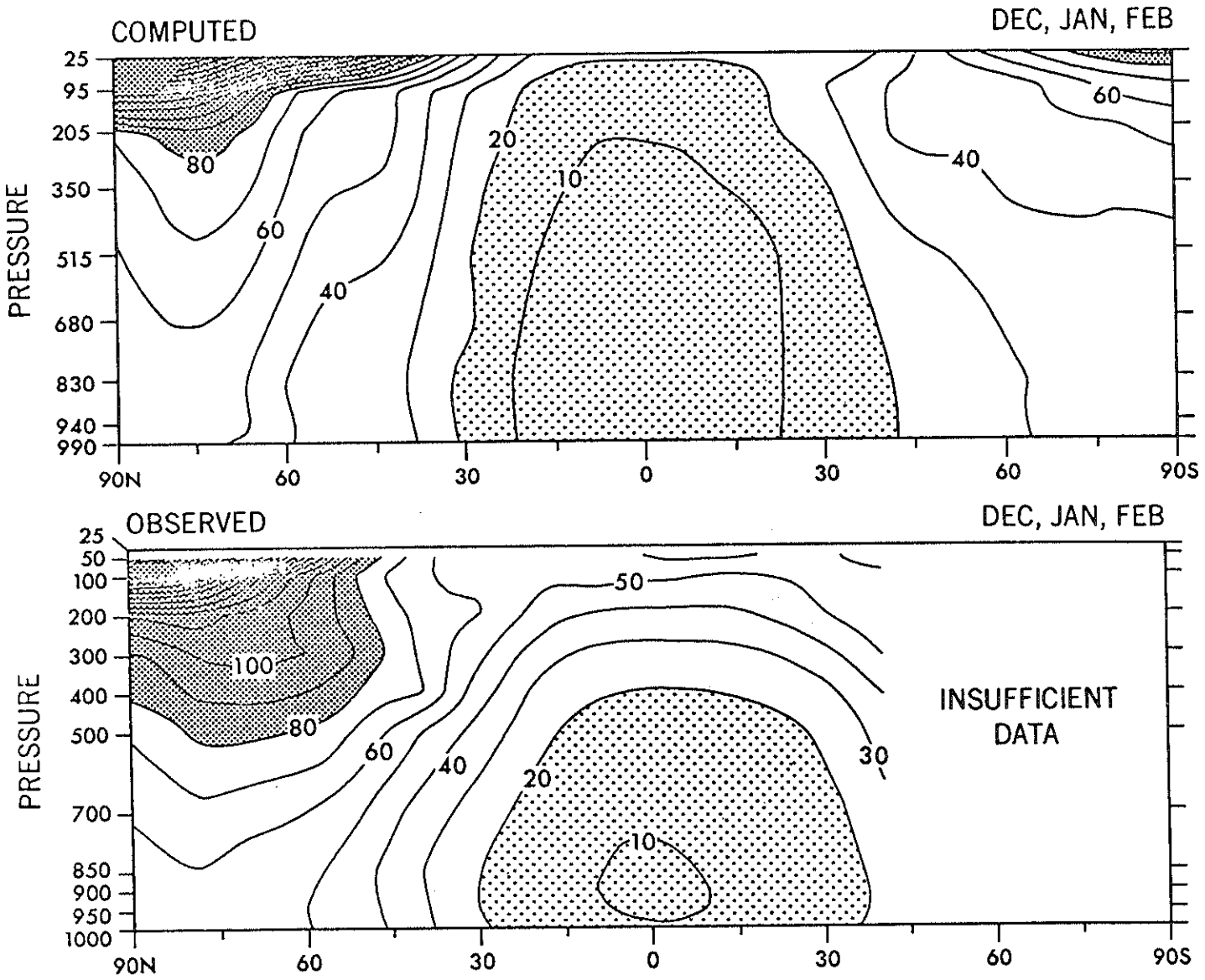

Figure 10b. Zonal mean of the standard deviation of monthly mean geopotential height (m) for the Dec.-Jan.-Feb. season. Top: simulated; Bottom: observed (from Manabe and Hahn, 1981).

Figure 11a. Ratio of the variances of observed January mean and the natural variability of January mean geopotential height at 500 mb.

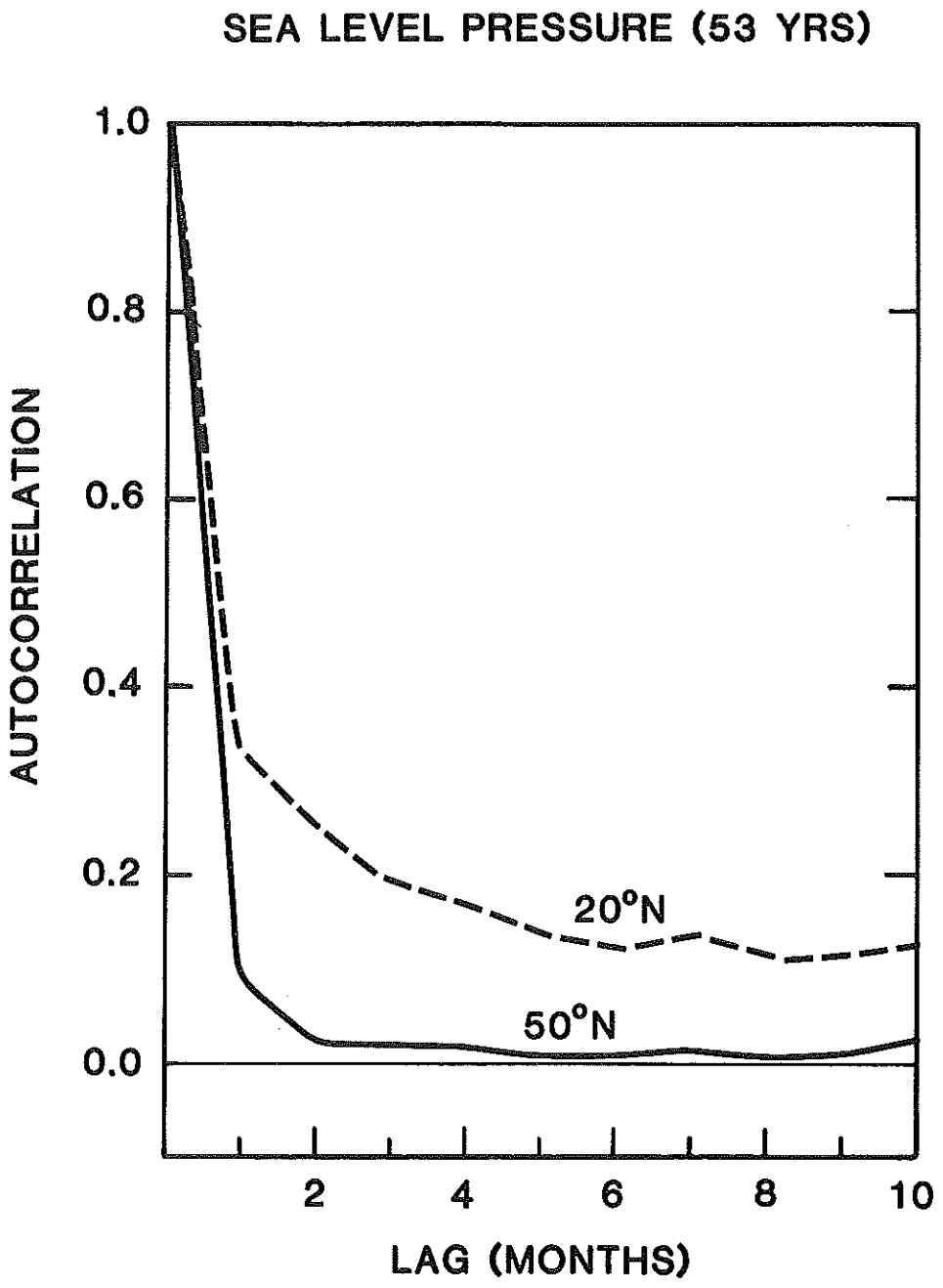

Figure 11b. Zonally averaged autocorrelation at 20°N and 50°N for monthly mean sea level pressure for the period 1925-77.